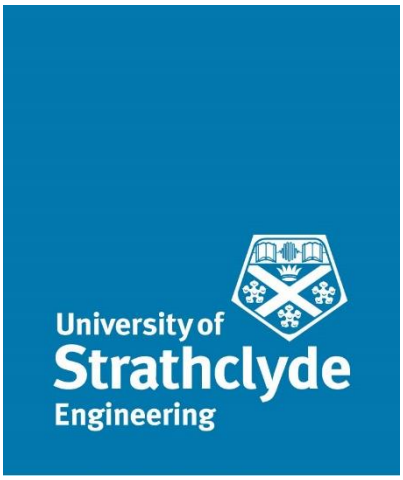

Department of Mechanical and Aerospace Engineering

Design and Analysis of Ground Source Heat Pump System associated with Grid Connected PV System in Multi-Family Building

Author: Agnieszka Bachleda-Baca

Supervisor: Dr Nicolas Kelly

A thesis submitted in partial fulfilment for the requirement of the degree

Master of Science

Sustainable Engineering: Renewable Energy Systems and the Environment

2018

Copyright Declaration

This thesis is the result of the author's original research. It has been composed by the author and has not been previously submitted for examination which has led to the award of a degree.

Signed:  Date: 23.08.2018

Abstract

Fuel poverty is a major problem in the social housing sector. Conventional electric heating in tower blocks isn't affordable for the tenants. On the other hand, low carbon economy requires transition from the fossil fuels to clean energy. Heat pumps are the fast-growing technology with big potential for energy saving and reduction of emission due to its high efficiency and using environment or waste as a source of heat.

Main aim of the project is a design and analysis of low-carbon affordable heat generation system. The project focuses on design of ground source heat pump, that delivers the heat required for space heating and domestic hot water usage, in a typical tower block residential building located in Glasgow. Additionally, the reduction of energy taken from the grid to drive the heat pump is considered by adding roof mounted PV system with energy storage.

Required space heating load was obtained from the Esp-r energy simulation results. Hot water load generated from the DWHcalc tool that uses a probability distribution function. The peak load for aggregated space heating and DHW was 377.4 kW and the total energy annual demand of 617.9 MWh. To reduce the peak load and capacity of the heat pump thermal storage was sized with total volume of 5000L. Chosen heat pump has COP of 4.76 and the heating output of 240 kW. As a heat for the heat pump comes from the ground, borehole heat exchanger total required length is 5807 m. Designed borehole fields has a pattern 8x8 composed from total 64 boreholes with a length of 91 m.

PV system composed from 150 modules made of polycrystalline silicone. The total installed power of the array is 35.3 kW. Total annual energy output for the Glasgow weather conditions estimated as 50242 kWh. For the storage purposes lead-acid batteries was chosen. The battery sized for daily energy output, assuming 1 day of autonomy. The total calculated capacity of battery bank is 9115AH, composed from 2 strings of 24 batteries. The battery bank connected to 10 connected in parallel charge controllers with charge current of 80A. electric output from batteries (DC) transformed to AC by 5 hybrid inverters connected in parallel with total output of 34 kW.

Financial analysis, based on payback period, net present value and internal rate of return, was performed for the 2 scenarios: 1) heat pump heat generation system 2) heat pump heating + grid connected PV array with storage. Project lifetime of 20 years was considered. The obtained payback period for both scenarios is similar above 5.05 and 5.47 years respectively. Calculated

NPV is higher for the Scenario 2 witch value of 1 415 317 £, comparing to 1 287 120 obtained for Scenario1. IRR values for both scenarios relatively close to each other, 28.11 and 25.49.

Environmental concerns of the project points to the possible environmental risks and evaluates positive impact on greenhouse gasses emission. Calculation shows that use of the heat pump heating reduces greenhouse gasses emission by 76% comparing to grid sources, conventional electric heating. Adding the PV system to the building with heat pump heating reduced emissions for another 35%.

Acknowledgment

I would like to thank the University of Strathclyde, course director Dr Paul Tuohy and all staff of ESRU for interesting coursework and valuable knowledge in the field of Renewable Energy Systems. Special thanks to my Supervisor Dr Nicolas Kelly for support and valuable suggestions during my work on project.

Very special thanks to all my classmates for their support, enthusiasm and good team work during coursework. It has been a pleasure to meet you all.

Table of Contents

List of Figures

List of Tables

List of Acronyms

Nomenclature

Q_g	Heat taken from the ground
Q_b	Heat delivered to the building
W_{net}	Power taken from the Grid
η_c	Compressor efficiency
COP_{HP}	Coefficient of Performance
$COP_{HP,Carnot}$	Carnot Coefficient of Performance
T_c	Temperature in condenser
T_e	Temperature in evaporator

η_s	System efficiency
Q_s	Quantity of heat stored
m	Mass flow
c_p	Specific heat of water
t_f	Final temperature
t_i	Initial temperature
L	Length
q	Heat load
Δt	Temperature difference between inlet and outlet
t, k	Timestep
ts	Time of storing
ρ	Density of water
R_t	Total thermal resistance
T_g	Ground temperature
T_m	Mean temperature of the fluid in the borehole
T_p	Penalty at the end of the month
L_i	Length of the borehole
$q_{h,i}$	Peak heat load for present month
$q_{pm,i}$	Average heat load for preceding month
$q_{cm,i}$	Average heat load for current month
R_b	Thermal resistance of the borehole
$R_{pm,i}$	Equivalent ground thermal resistance for preceding month
$R_{cm,i}$	Equivalent ground thermal resistance for current month
$R_{h,i}$	Equivalent ground thermal resistance for peak load month
$prob$	Probability
$\dot{V}$	Volume flow
$\dot{V}_{mean}$	Average volume flow
σ^2	Variance
p	Probability function

p_{day}	Daily probability
$p_{weekday}$	Weekly probability distribution
p_{season}	Seasonal probability distribution
$p_{holiday}$	Holiday probability distribution
I	Integral
$V_{w,day}$	Total daily requirement for hot water in the tower block
N_F	Number of floors in the building
N_H	Number of flats on each floor
n	Number of occupants
$v_{w,day}$	Hot water demand per person
Q_{DWH}	Heat load required for domestic hot water preparation
$\mathrm{V_{DWH}}$	Volume floe rate of the hot water
n_{seg}	Number of segments
$n_{ts,seg}$	All elements in the segment
P_{tes}	Heat in the storage
P_{gen}	Heat input to the store
P_{dem}	Thermal demand on the store
E_{tes}	Energy required in the Storage
E_{dem}	Energy demand
E_{losses}	Energy losses
Q_{tes}	Capacity Required in the Thermal Store
$Q_{tes,q}$	Required Capacity of Storage for the segment
$Q *_{tes,q}$	Storage capacity for perfectly insulated Store
$E_{losses,24h}$	daily energy looses
$V_{tes,q}$	Volume of Storage for the segment
Q_e	Heat output from condenser
W_{comp}	Power consumed by the compressor
$Q_{mean,i}$	Average heat demand
$Q_{peak,i}$	Peak heat demand

Q_{HP}	Nominal capacity of heat pump
G	G-factor for the cylindrical source
Fo	Fourier Number
d	Borehole diameter
α	Ground thermal diffusivity
q_i	Average ground load up to that point
λ_g	Ground conductivity
g	g-functions generated for specific D, rb, H, nb and B of the borehole
D	Buried depth
rb	Borehole radius
nb	Number of boreholes in the borehole field
B	Borehole spacing
t_s	Nondimensional time
H	Height of the borehole
$E_{HP,m}$	Monthly diurnal energy required to drive the heat pump
$Q_{d,i}$	Heat demand for i-th timestep
$E_{HP,a}$	Total annual energy required to drive the heat pump
η_{pv}	Efficiency of PV cell
η_{STC}	PV efficiency in standard test conditions
β_P	Solar cell temperature coefficient
T_c	Solar cell temperature
γ	irradiance coefficient
I_{tot}	Solar irradiance
T_a	Ambient temperature
T_{NOCT}	Nominal operating cell temperature

I_{dh}	Direct horizontal irradiance
I_{fh}	Diffuse horizontal irradiance
I_{dn}	Direct normal irradiance
I_{gh}	Global horizontal irradiance
β_s	Elevation
β_f	Inclination
$I_{d\beta}$	Direct irradiance on inclined surface
i_β	Angle of incidence
$I_{r\beta}$	Ground reflected irradiance on inclined surface
rg	Ground reflectance
$I_{s\beta}$	Sky component of irradiance on inclined surface
ω	surface-solar azimuth
α_s	solar azimuth
α_f	surface azimuth
P_{pv}	power output from solar module
$E_{pv,d}$	Daily energy output from solar module
$E_{pv,a}$	Total annual energy output from PV system
n_{pv}	Number of solar modules in the array
$E_{el,d}$	Required daily electricity load
$n_{pv,max}$	Max. number of modules in the array
$E_{array,m}$	Monthly energy output from the solar array
$E_{pv,d,month}$	Average daily energy output for specific month
η_{inv}	inverter efficiency

$P_{n,array}$	Nominal installed power of an array
C_b	Capacity of the battery bank
E_{load}	Daily average load for summer month
d	Number of days of autonomy
V_b	Battery bus voltage
DoD	Depth of discharge
η_B	Efficiency of the battery
V_{oc}	Open circuit voltage
$V_{oc,max}$	Max PV array open circuit voltage
I_{ch}	Rated charge current
V_b	Nominal battery voltage
C_0	Initial Investment
C_{income}	Cash in-flows
C_i	Cash Flows
r	Discount rate
T	Year of the project
I_{cost}	Investment cost
G	Cost of generation
Rhi	Renewable Heat Incentive income
S	Savings in energy cost
$G_{el,a}$	Annual cost of conventional electric heating
$E_{h,a}$	Annual energy demand for heating
$G_{hp,a}$	Annual cost of heat pump heating
i	Inflation rate

n Equipment lifetime

L_r Annual leakage rate

m_r Refrigerant charge

GWP Global Warming Potential of refrigerant

E_{annual} Annual Energy Use

EF Emission factor of driving energy

$L_{demolition}$ Refrigerant Losses during Demolition

1. Introduction

1.1. Background

Over 400,000 homes in the UK are based in tower blocks which are most often a social housing stock. Social housing is defined is defined as affordable housing for people on a low income. Most of high-rise tower blocks in the UK do not have gas central heating and the heating is based on electric storage radiators. With the time cost of conventional electric heating significantly increased leaving the tenants facing the fuel poverty. On the other hand, UK is in the transition to low carbon economy requires use transformation from the fossil fuels systems to low carbon solutions. Decarbonisation of the energy systems is a main goal and the heating sector is most challenging. In the UK about 80% of energy in dwellings is spent for heating requirements which is now supplied mainly by gas. Decarbonisation of electric grid and electrification heating is seen as the most likely path for the domestic sector. That raises the question what will going to happen with the fuel poverty issue. The demand is the largest factor affecting electricity price and with heating electrification demand will only rise which means the fuel poverty could become even more challenging. Modernisation of the heating system in the high-rise residential buildings is highly required. The most popular alternative system adopted in UK is district heating system which certainly is a good solution for bigger housing estates, but a diversity of systems should be introduced in a country scale.

Image 1 Residential Tower blocks

1.2. Aims and Objectives

The project is a feasibility study of alternative to district heating, building integrated system. The concept includes a design of ground source heat pump generation system for heating and domestic hot water. Additionally, PV system was considered to reduce the energy load needed from grid to drive the heat pump. Financial analysis was performed to check the profitability of 2 different configurations of system, one with heat pump heating system and another with heat

pump and associated PV generation. Environmental concerns of the project were considered as a part of the study and included in the overall summary of the project.

The representative building used as a case study is existing high-rise residential building in the West Whitlawburn area of Glasgow. Currently the building is connected to biomass district heating system, however before that was implemented it was using electric storage and panel heating. I have used that building to investigate my proposed solution as an alternative not replacement for the current biomass system, hence economic analysis is based on savings on energy compared to the conventional electric system. Outcomes of the project should help to answer the question if the building integrated heat pumps accompanied by PV system can work is a good solution for the multi-storey buildings, in the terms of energy savings as well as financial and environmental aspects.

1.3. Methodology

The following Figure 1shows the Phases of the project in order.

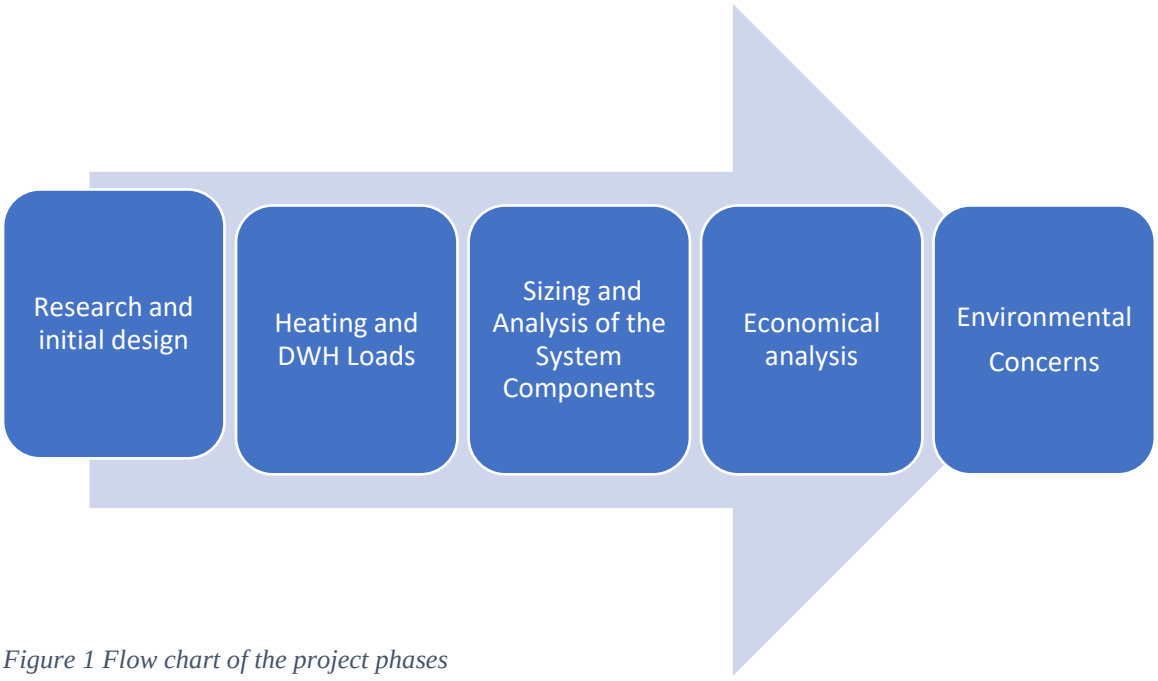

Figure 1 Flow chart of the project phases

Phase 1 -Research and Initial Design

Initial design phase started from choosing potential location for PV and GHE considering the available space and environmental conditions. After that the specific technology was chosen.

Phase 2 -Heating and DHW loads

ESP-r tool was used to create model, run the simulation and obtain the space heating profile for one floor of the building which was then scaled up for all 12 floors. Hot water profile was modelled using another software DWHcalc.

Phase 3 -The design process of the system component was based on the analytical calculation methods adopted from the reference literature. Details of those approaches are presented in the Design chapter. The calculations were implemented in the Excel spreadsheet and validated using manual calculations

Phase 4 -Financial analysis is based on 3 scenarios of different system configuration. Evaluation is based on the common project profitability indices (PP,NPV,IRR) calculated using the Excel spreadsheet.

Phase 5- Environmental value of the project is approached in the form of discussion related to emission reduction, considering possible environmental impacts and mitigation that could be used.

2. Literature Review

2.1. Fuel Poverty in Scotland

According to the latest published house condition survey (Figure 2) in 2016 around 74% household energy demand was from space heating and another 13 % from water heating. Energy usage is dominated by the heating requirements, which is common trend for the countries with colder climate. The fuel used for heating and its prices, as well as the energy efficiency of the building, play a key role in the costs paid by end user.

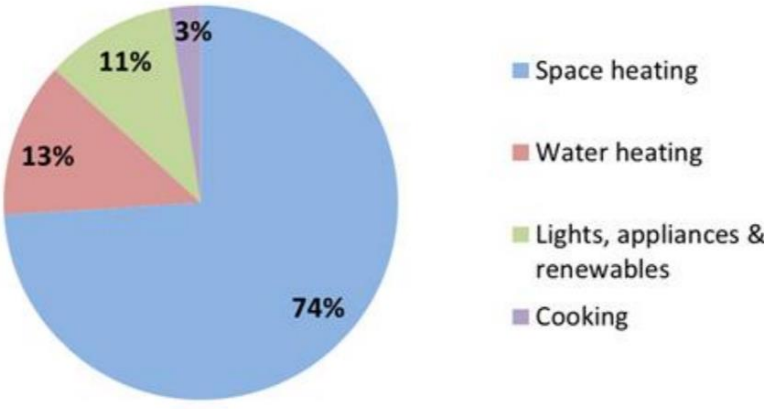

Figure 2 Mean household energy consumption by end user, 2016 [2]

Referring to the Scottish Government a person is living in a fuel poverty, if in the order to maintain satisfactory heating requirements, more than 10 % of the household total income need to be spent on the fuel use. If the household would have to spend more than 20% of its income that classifies as an extreme fuel poverty [1].Figure 3 Shows how the fuel poverty rate changed in the period from 2011 to 2016. The rate declined by about 4% however the numbers was still quite high: 26.5% which is 649,000 households suffering fuel poverty and 7.5 %, about 183,000 affected with extreme fuel poverty [2].

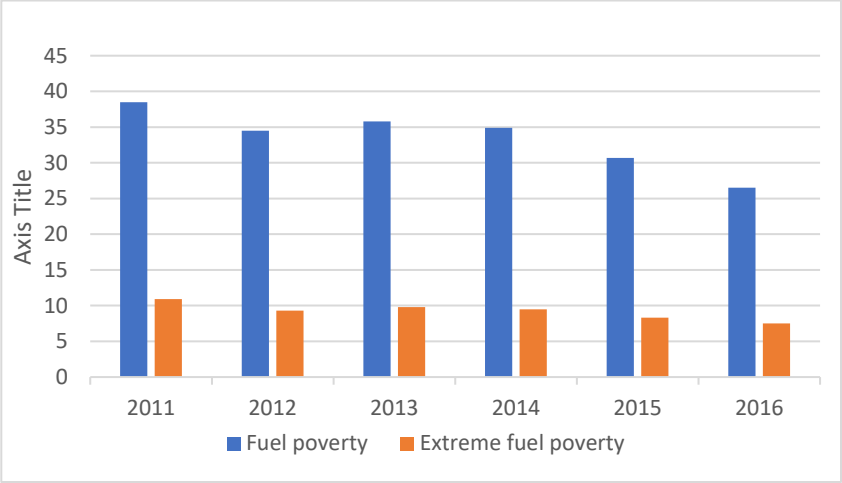

Figure 3 Fuel poverty and extreme poverty rates

Fuel poverty can be caused by 3 main drivers, or its combination drivers, which are: price of fuel, energy efficiency of the housing and the household income. According to the Figure 4 fuel poverty trend follows the fuel prices which have risen significantly by 2016 for about 155%, while the median income has increased only for about 39%. It is noticeable that the price has the strongest influence on the fuel poverty.

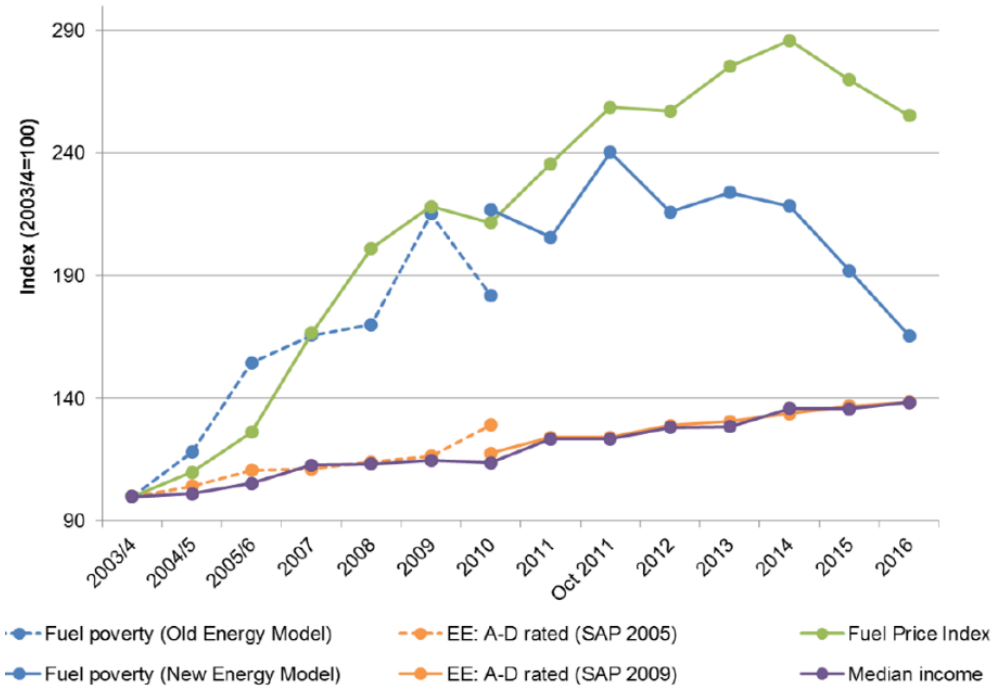

Figure 4 Trends in Fuel Price and Median income [2]

Between 2015 and 2016 fuel poverty fell. The reports from micro-simulation analysis showing that most of the reduction came from the lower price of fuels in 2016. That was mainly caused by drop in prices of gas and liquid fuels in that period. The remaining other factors were improved energy performance and higher household incomes.

Characteristic of households shows that 10 % of households in fuel poverty are families with children, remaining 90% are split between one or two-person households. Large majority of poor households are owner occupiers (58%), on second place is the social housing sector (31%) and the private sector (11%). 70% of fuel poor people live in houses and remaining 30 % occupy flats.

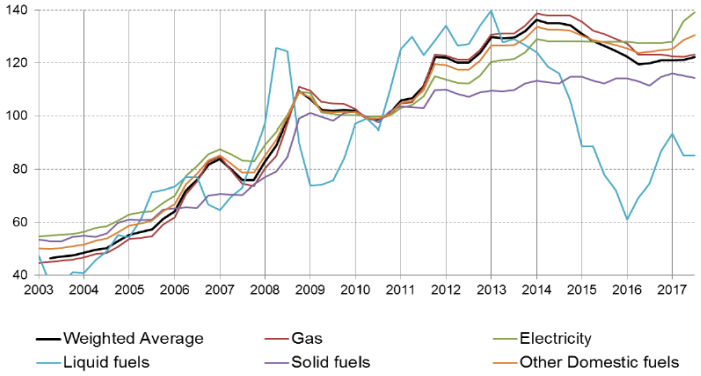

Figure 5 Price indices for different heating fuels [2]

According to the average index value for the heating fuel price (Figure 5) the electricity prices have increasing trend which may indicates that the risk of fuel poverty is bigger for the households with conventional electric heating. The characteristic presented in the report compares the fuel poverty rates against the primary heating fuel and electricity have the highest 51% rate. Another, heating satisfaction survey, included in the paper confirms that

most unsatisfied tenants are the one that use electric heating as the primary fuel as well as the social housing tenants were less satisfied from the heating and the most often reason given was poor or inadequate heating.

The impact of fuel poverty can be rather serious and leads consequences such as discomfort, increasing debts and bad health and. Very often people who struggle to pay their bills choose to limit the heating their use and live outside the thermal comfort zone. Cold and dump living environment can cause several health issues such as: asthma, bad heart condition, weak immune system and depression.

2.2. Role of Heat pumps in Low-Carbon Economy

Low carbon economy was first proposed by the British government in energy white paper in 2003. 2 years later the ministers of environment and energy from 20 countries participated in the meeting discussing how to move to low-carbon economy [3]. Since then the concept spread all over the world and became important step towards achieving sustainable development. Affordable and clean energy is one of the main goals adopted by 150 world leaders at The United Nations Sustainable Development Summit in 2015 [4]. Different countries developing the strategies for shifting towards clean energy.

For colder countries more energy in houses is used for heating requirements. Karl Drage in his lecture talked how the energy to heat house going to be lot more expensive due to low carbon economy [5]. Currently, subsidized by government, gas price will eventually rise due to carbon tax which will boost shift to alternative heating in dwellings, most likely electric. Electricity demand will therefore increase, and the cost-effective technologies will play very important role. There is no doubt that delivering of space heating and hot water to dwellings need to be reconsidered taking as a main goal: reduction of carbon emission, shifting from dependence on gas and finally tackling problem of rising energy prices and fuel poverty.

To promote renewable heat and reduce carbon emission UK government introduced Renewable Heat Incentive (RHI) is a scheme implemented across UK to encourage a switch from fossil fuel heating systems to renewable and low-carbon technologies. It provides financial support to the owners of renewable energy systems in the form of fed-inn tariff for renewable heat produced. The program supports heat pump systems recognising it as renewable heat supply.

Heat pump are fast growing technology and are seen as key technology for decarbonising water and space heating in such countries like Sweden and Denmark. The heat pump technology is

relatively flexible and can be applied to the district heating systems, industry or as building integrated solution. The potential energy and CO2 savings are substantial from the wider use of heat pump due to high thermal efficiency (COP=3 to 6). It's a growing opportunity to oppose the fuel poverty issue caused by rising energy prices. The efficiency of heat pumps has increased during past years due to technical and control system improvements. Seasonal performance factor (ratio of energy delivered to consumed in the heating season) reaches the level 6-7. Heat pumps can be also combining with the thermal storage to reduce peak power demand or with other renewables such as PV modules which can help to reduce energy supplied from the grid. Major barriers to reduce widespread of heat pumps are high investment costs and insufficient recognition of benefits [5].

According to the IRENA study of the future potential of renewables in Europe there is significant advantages in deployment of heat pumps- which could account for about 9% of heating needs by 2030 in industry and buildings. The potential for heat pump is seeing as cost-effective solution for decarbonized heat in buildings. Looking at one of the future scenarios the power generation and building would see the biggest percentage reduction in emission by 2050 and the role of heat pumps for space heating and water heating would grow rapidly [6].

2.3. Overview of Heat Pump Technology

2.3.1. Operation and Thermodynamics

Heat energy natural flow is from hot to colder space. Main operation of heat pump is opposite to that as it moves the heat energy from colder to hotter space and additional energy is required to achieve that. There are basically 2 sides: low temperature heat source and the sink where the heat is sent and used. Heat can be taken from environment (ground, water, air) or process waste heat (air, water). Heat pump can operate using refrigeration or absorption cycle. This paper focus on devices that use refrigeration cycle.

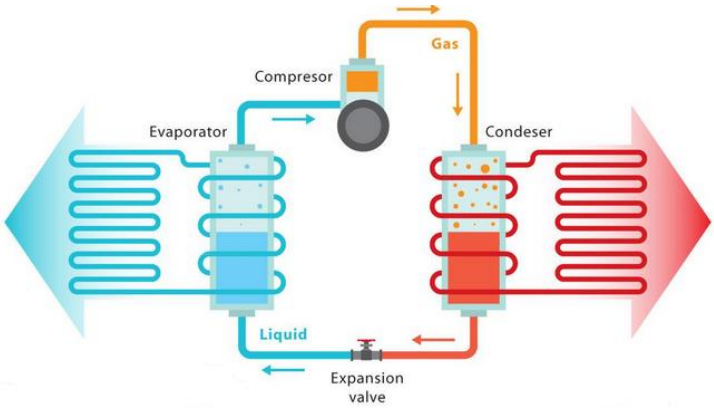

Figure 6 Operation of the heat pump [71]

The main components of refrigeration cycle are evaporator, condenser, compressor and expansion valve (Figure 6). Thermodynamic processes can be illustrated on the pressure-enthalpy diagram for specific refrigerant shown on Figure 7. Liquid refrigerant passes through the evaporator and absorbs heat from the low temperature source and the refrigerant is vaporised. Compressor raises the pressure, which is accompanied by temperature increase, hence the energy content (enthalpy) increases. In the next stage the refrigerant flows through the condenser where it transforms from vapor to liquid form. During this change environmental energy that has been absorbed from environment plus the energy drawn by compressor is released. Condensed refrigerant flows through the expansion valve and its pressure is dropped to the original state accompanied by temperature drop. The refrigerant goes back to evaporator and cycle starts again [7]. The heat pump cycle can be reversed by using special valve to reverse the flow, so it can operate in cooling mode.

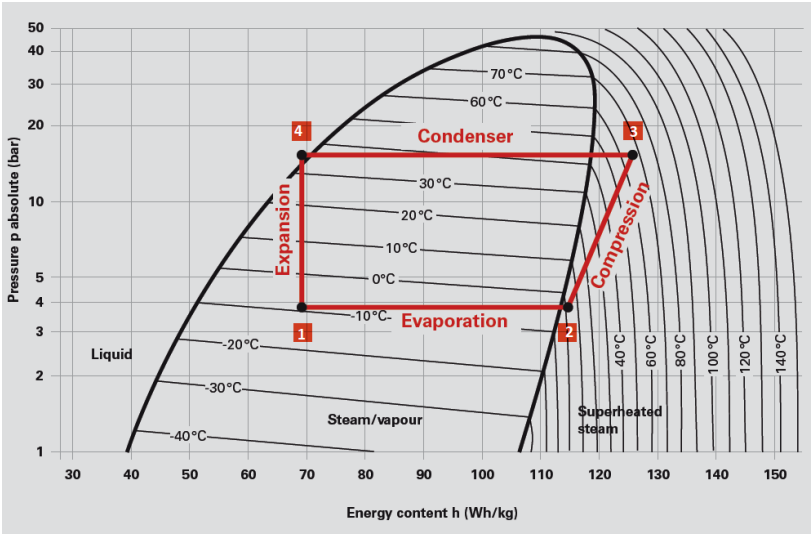

Figure 7 Changes of state in refrigeration cycle of heat pump [7]

There are 3 main types of heat pump considering the source of heat:

- Ground source – energy is extracted from the soil trough the vertical or horizontal heat exchanger
- Air source energy extracted from the external or waste heat
- Water source- energy extracted directly from the environment (sea, river etc.) or waste water

There are also different possible configurations of the heat pump depending on the medium and heat exchangers: air to air, water to water, air to water, water to air.

2.3.2. Energy Balance and Efficiency

Heat taken from the ground Q_g is the heat that is absorbed in the evaporator of the heat pump. While the Q_b is the heat released in the heat pump condenser and delivered to the building. External energy is consumed by the compressor.

From the 1st law of thermodynamics the energy balance:

$$W_{comp} + Q_g = Q_b$$

Work input to the compressor is:

$$W_{comp} = \frac{W_{net}}{\eta_c}$$

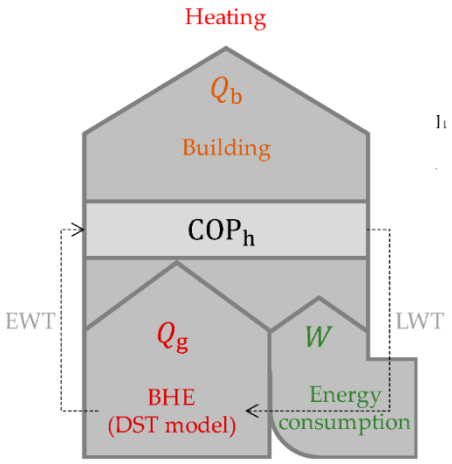

Figure 8 Energy balance of the heat pump for the heating cycle [57]

η −efficiency of compressor

The classic parameter describing the performance of the heat pump is:

$$COP_{HP} = \frac{Q_b}{W_{comp}} = \frac{Q_b}{Q_b - Q_g}$$

Max theoretical efficiency of heating process is expressed by [8]:

$$COP_{HP,Carnot} = \frac{T_c}{T_c - T_e}$$

T_c − absolute temperature of the hot side

T_e −absolute temperature of the cold side

Real COP can be calculated from Carnot and the system efficiency

$$COP_{HP} = \eta_s * COP_{h,carnot}$$

2.3.3. Thermal Storage for demand-site management

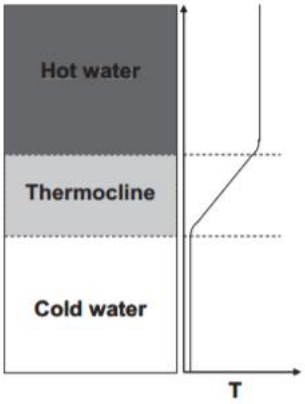

Figure 9 Stratified storage tank [10]

Electrification of heating seen as the most likely scenario for the UK could significantly increase electrical demands variation and the thermal storage is seen as a way to mitigate the impact on the grid by managing when the energy is drawn from the grid and when the heat is supplied to the end users [9]. According to the definition demand site management is an instrument that focuses on changing the load profile to optimize power system from generation to the end user. Thermal Energy storage (TES) is recognised as the component that integrates renewable energies into electricity production on the generation side, however, it can be used as well on the demand side. TES have capability to shift electrical loads from high peak to off-peak hours [10]. Particularly it is used for thermal applications where heating and cooling are produced electrically, heat pump is a perfect example of that kind of system. In the configuration with heat pump TES system can helps to reduce the power output from the device in the high peak hours or entirely shift the load to the off-peak hours. The basic principle of operation is based on charging, storing and discharging at high demand time. There are 3 types of TES that can be used: sensible, latent and thermochemical heat storage. For the heating systems integrated in the building where the thermal load is produced electrically sensible heat storage with stratified storage tanks have been widely used (Figure 9).

Sensible heat storage relies on the storage of heat in a solid or liquid with no phase change or chemical reactions taking place. The materials with high density and specific heat capacity can store larger amount of heat compared to those with lover values. To charge the storage heat is added from higher temperature source resulting in a temperature rise in the store. During discharging the heat is extracted to allow temperature sink and the storage temperature is reduced. For a storage with specified medium, density and specific heat capacity the heat stored scales linearly with store volume and temperature difference. Energy losses from store, for given U-value of the wall, are proportional to the store surface area and temperature difference between the store and ambient environment [11]. The amount of heat stored depends on the specific heat of the medium, temperature change, and the amount of storage medium

$$Q_s = \int_{t_i}^{t_f} mc_p dt = mc_p(t_f - t_i)$$

Q_s −is the quantity of heat stored m −mass flow of the stored medium, c_p −specific heat, t_i- initial temperature, t_f − final temperature?

2.3.4. Ground Source Heat Pump Systems

Ground-source heat pump use the ground as a heat source to provide space heating and domestic hot water. They have higher efficiency than air source heat pump due to fairly constant ground temperatures below the frost line. Basically, on winter the ground temperature is higher than outside air. Ground heat pump system is composed from 3 main elements: ground heat exchanger, heat pump and distribution system. Available systems are grouped into three categories: ground water, surface water and ground-coupled heat pumps.

Surface water systems can be closed loop or open loop with water-to-water or air-to-water heat pump. SWHP is usually linked to the piping network placed in water reservoir or river. A pump circulates antifreeze-water mixture through the heat pump's water to refrigerant coil and the heat is transferred from the water to the evaporator. Some advantages of that system are: lower cost compared to ground coupled systems, low pumping requirements, low maintenance, high reliability and low operating cost. The major disadvantages are possibility of coil damage in the public water reservoirs and big temperature fluctuations with outdoor condition if the reservoir is small and shallow, which affects the efficiency of the heat pump.

Ground water system removes groundwater from a well and delivers it to a heat pump. The advantage of GWHPs are lower costs compared to ground coupled systems, water well is very compact and water well contractors are widely available. That technology has been also used for decades. Disadvantages are the water availability may be limited, fouling precautions may be necessary if the well is not properly developed or water quality is poor, pumping energy might be excessive if the pump is oversized or poorly controlled [12].

Ground Coupled Systems uses the renewable storage capacity of the ground as the heat source or sing to provide space heating, cooling and domestic hot water. Ground coupled heat pump system are often referred to closed-loop ground source heat pumps. The system consists of heat pump that is linked to, buried in the soil, heat exchanger. There are few designs of ground heat exchangers that can be installed: vertical bore ground loops, horizontal bore ground loops and trenched horizontal ground loop (Figure 10)

From available technologies GCHP seems to be most reliable as the application of two other can be restricted by factors such as: limited availability of groundwater, corrosion or low temperature of surface water on winter. Vertical heat exchangers are the most common types due to relatively small plots of ground required, small variations in soil temperatures and thermal properties, smallest amount of pipe and pumping energy. Comparing to horizontal type it is more efficient system, but the installation costs are higher. Horizontal heat exchangers are typically less expensive than vertical in smaller applications, but larger area of ground is required. The other disadvantage is bigger variations in performance caused by fluctuation of ground temperatures and thermal properties during the winter season. Higher pumping energy required, and the system have smaller efficiency. Vertical heat exchanger is recommended for bigger applications [12]

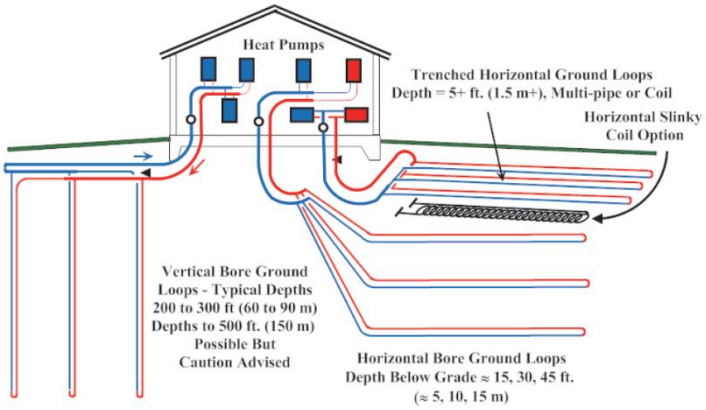

Figure 10 Ground -Loop option for GCHP system [12]

2.4. Vertical heat exchanger

In geology the shallow geothermal or ground-source means the area from surface up to 400 m. This is the area where the vertical heat exchanger can be placed. Figure 11 shows profile of annual ground temperature level up to 20 m and beyond. It's noticeable that at the depth 1.2-15m temperature fluctuates between 7 and 13 ℃ through the different seasons of the year. At 18 m temperature is about 10 ℃ all year round. Typically, the temperature increases every 100 m by 2 to 3 ℃ [13].

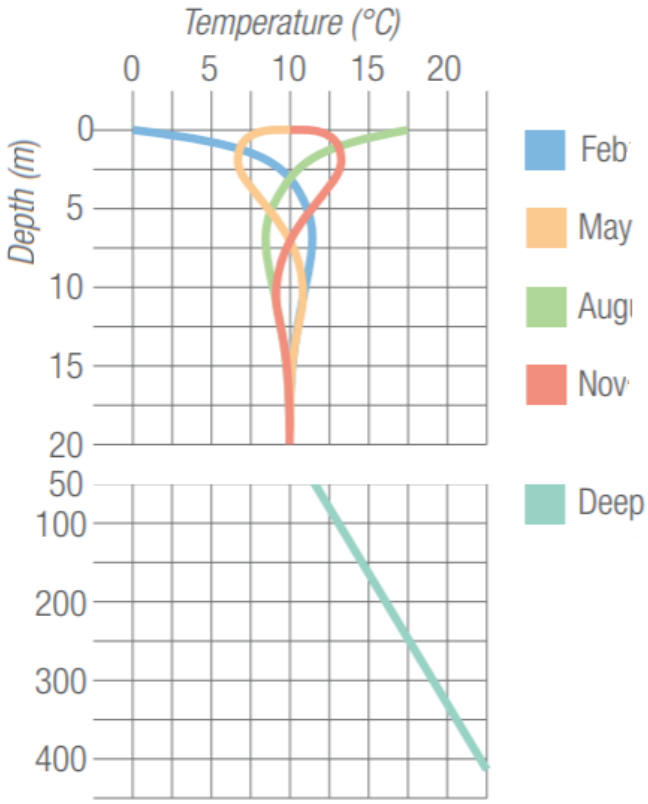

Figure 11 Annual temperature level at various ground depth [13]

There are 3 types of vertical heat exchangers that can be used: ground-source U-probes (BHE), coaxial probes, energy piles, helix.

U-probes are installed usually at a depth up to 300 m in order to take advantage from constant temperature at deeper layers.

U-tube ground heat exchanger may include multiple boreholes depending of heating load. Typical U-tube have nominal diameter 20-40mm and length 20-200 m. The borehole is backfilled with the grout to prevent contamination of groundwater as shown on the Image 2 . The tubes are filled with antifreeze brine solution and can have simple or double configuration. The basic equation in steady state is noted as [12]:

$$L = \frac{q * R_t}{(T_g - T_m)}$$

That can be modified to represent variable heat rate by using a series of heat rate pulses. The length of the required borehole can be calculated from the formula

Image 2 Insulated probes [13]

proposed by Bernier and modified to monthly based methodology [14].

$$L_i = \frac{q_{h,i} * R_b + q_{pm,i} * R_{pm,i} + q_{cm,i*} R_{cm} + q_{h,i} * R_{h,i}}{(T_m - (T_g + T_{p,})}$$

Where: $q_{h,i}, q_{pm,i}, q_{cm,i}$ −peak and average loads for preceding and present month, $R_{cm}, R_{pm,i}, R_{h,i}$ −effective ground thermal resistances for preceding and present month, Rb-thermal resistance of the borehole, T_m −mean temperature of the fluid in the borehole, T_g −undistribuited ground temperature, T_p −temperature penalty at the end of the month. The calculation of various loads illustrated on Figure 12.

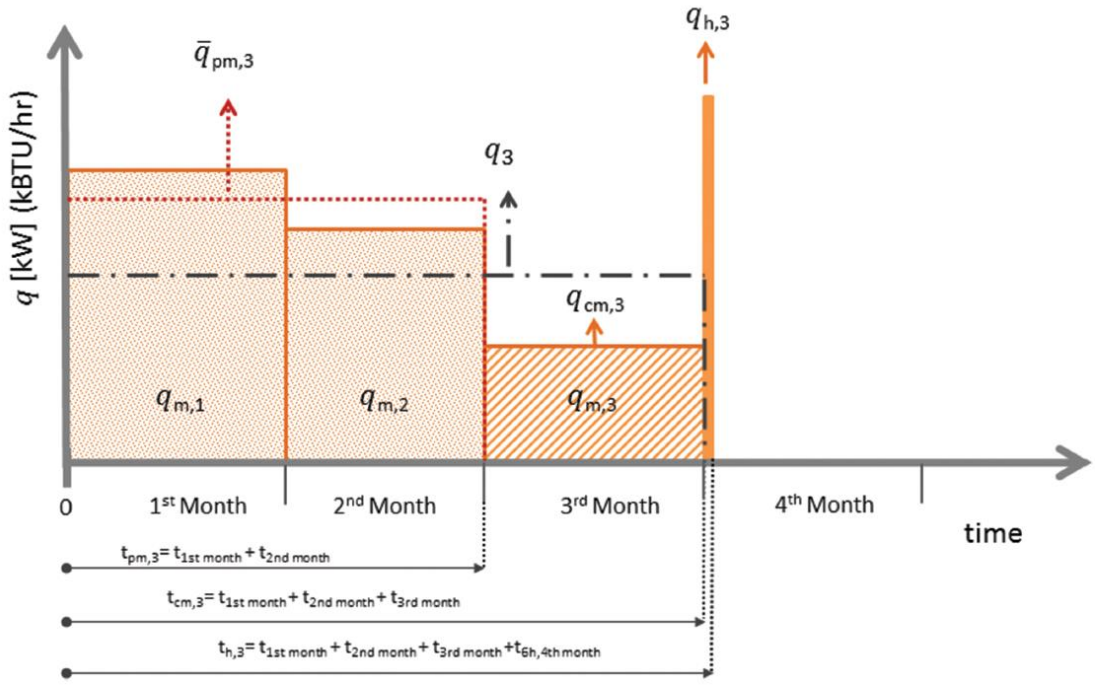

Figure 12 Calculation of various loads [14]

2.5. Overview and operation of PV systems

2.5.1. Basic principles

PV module is composed from multiple solar cells. Solar cell is a solid-state electrical device that can convert energy of light directly into electricity using a photovoltaic effect. Typical PV cell is composed from thin wafer consisting of an ultra-thin layer of N-type silicon on the top of the thicker layer of P-type silicon. Electrical field is created near the top of the surface of the cell where those materials are in contact, called P-N-junction. Sunlight strike the surface of a cell and the electric field provides momentum and direction to light stimulated electrons which results in a flow of current when cell is connected to electrical load [15]. PV cells are connected in series or parallel circuits to produce higher voltages, current and power levels.

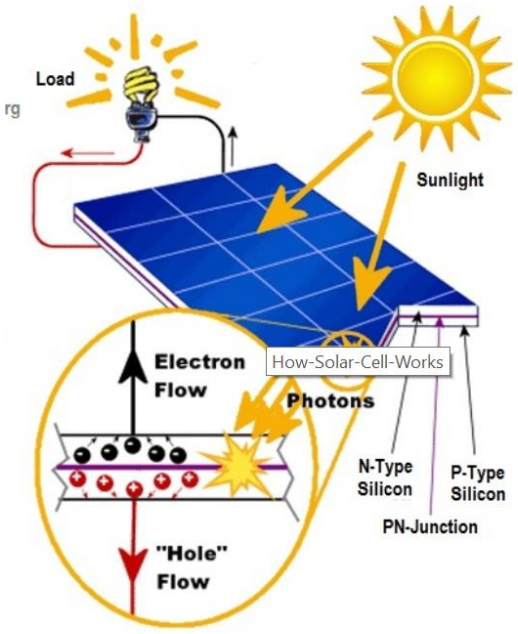

Figure 13 Operation principle of solar cell [15]

Typical silicon PV cell produces about 0.5-0.6-volt DC. Power output of a PV cell depends on its efficiency and surface area. It is proportional to the intensity of solar radiation on the cell surface.

Performance of PV modules is rated by producers according to the max DC power output under Standard Test Conditions. STC are defined by temperature 25°C and irradiance 1000W/m^2. Actual performance is usually lower than STC rating.

2.5.2. Types of the Systems:

- Grid Connected PV System

Designed to operate in parallel with and interconnected with the electricity utility grid. The primary element is the inverter that converts DC power produced by PV array into AC power consistent with the voltage and power quality requirements of the utility grid. Bi-directional Interface is made between the PV system AC output and the electricity grid at

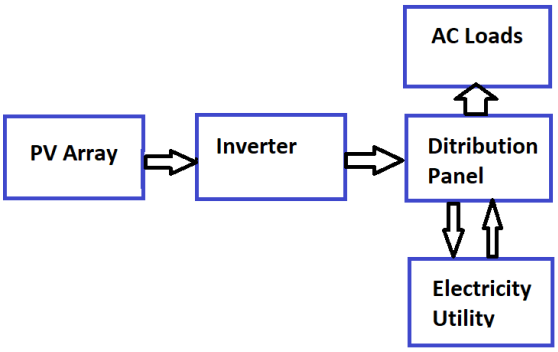

Figure 14 On-grid PV System

on-site distribution panel. AC power produced by PV is either supplied to the electrical loads or feed in to grid when the PV system output is grated than the on-side load demand (surplus energy). At nigh time and during the periods when electrical load is greater than the PV system output the extra amount of power required by the load is supplied from the grid [15].

- Stand-Alone PV System

That kind of system is designed to operate independent from the electricity grid. It consists PV array, storage batteries, charge controller and inverter. Storage batteries store the electrical energy for use when solar isn't available. Charge controller regulates and regulates output from the PV array to prevent overcharging of the batteries. Inverter DC to AC power. DC loads can also be connected to the battery bank [16].

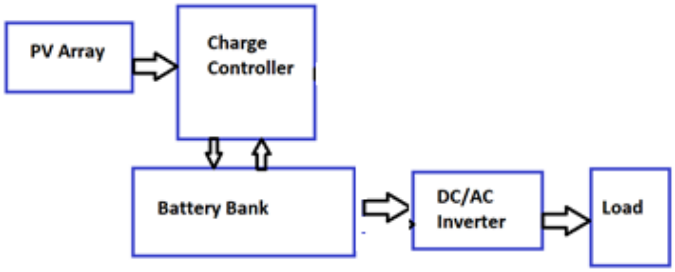

Figure 15 Off-Grid PV System

- Hybrid Solar System

The system combines off-grid solar with grid-connected systems. This system is less expensive than off-grid system as the batter bank can be downsized. System have the ability to charge the battery bank and provide electricity when weather conditions are unfavourable for solar power production. When there is not enough power produced from PV array and stored in the battery bank the system can also use the energy from grid [16].

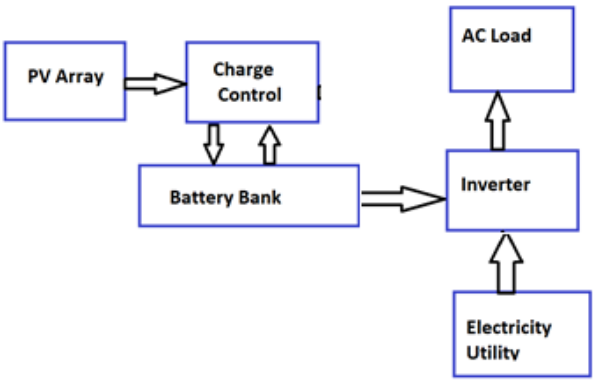

Figure 16 Hybrid PV System

2.5.3. Types of PV cells

There is variety of cells on the market, but the most common types are those made of crystalline silicon and so-called thin film technology. The majority, about 90% of all solar cells are made from crystalline silicon. However, the silicon

can take many different forms. They are distinguished by the purity of silicon (the way in which silicon modules are aligned). The grater purity of the silicon, the higher efficiency of the cell. Thin film solar technology represents approximately 7 % of global market. Thin film is characterized by various semi-conducting materials layered on top of another to create a series of thin films [17]. The characteristic of main types of cells summarised in the Table 1.

Table 1 Characteristic of solar cells

Silicon Solar Cells		
Monocrystalline Cells	Made from very pure type of silicon. Manufactured from single crystal ingot cut into slices. Shaped cylindrically which helps optimize the performance. From all types of cells, they take least space amount relative to generation intensity. They last longest of all types of cells, up to 25 years. The most efficient silicon cells but also the most expensive of all available types.	Up to 20 %
Polycrystalline Cells	First type of cells ever invented. The silicon is melted and shaped into square cells. They are much more affordable since hardly any silicon is wasted during the manufacturing. Material have lower purity than monocrystalline therefore lower efficiency. It also has lower heat tolerance which means that don't perform as efficient in higher temperatures.	13-16%
The Film Solar Cells		
Amorphous Cells	Made from amorphous silicon (non-crystalline, allotropic) It has high absorption capacity and can be used for cells with small layer thicknesses. This	Up to 13 %

	kind of silicone can be deposited at very low temperatures and on various structures. It's used for small applications such as watches, pocket calculators.	
Cadmium Telluride Cells	Lower cost alternative to crystalline silicone technologies. The material has very high absorption rate and manufacturing cost are low. Cadmium is a toxic material, so the disposal and long-term safety is known issue in large-scale applications.	Up to 15%
Copper Indium Gallium Selenide Cells	Comparable to crystalline technologies. Material have favourable electronic and optical properties. However, they still in the stage of research and testing. They have not been commercial deployed on any wide scale	12-14%

2.5.4. Characteristic of Batteries

According to information taken from the website [18] the characteristic of batteries and different types was summarised in this chapter.

The function of batteries is to balance outgoing electrical requirement with the incoming power supply. Mainly used in off-grid systems however, can be also used for grid connected systems to allow surplus energy to be stored to enable grater 'self-consumption' of generated energy. Critical battery characteristics or specification include battery voltage, capacity, charging/discharging regimes, depth of discharge efficiency and lifetime [19].

Battery capacity is the max. amount of energy that can be extracted from the battery. The actual storage capabilities can vary significantly from nominal, as it strongly depends on the age and charge/discharge regimes of the battery and temperature. If the battery is being discharged very quickly because of high discharge current, then the amount of energy that can be extracted from the battery is reduced and the battery capacity is lower. Alternatively, if the battery is discharged

at very slow rate using a low current, more energy can be extracted from battery and the battery capacity is higher. Temperature of battery also affect the energy output. At higher temperatures the battery capacity is typically higher than in lower temperatures. However, the temperature also decreases the battery lifetime. Age and history of battery can also decrease the capacity [18].

Some types of batteries cannot be totally discharged without causing serious damage to the battery. The Depth of Discharge (DOD) determines the fraction of power that can be withdrawn from the battery. Depends on the type of battery extracting the full battery capacity could dramatically reduce battery lifetime. Each battery has particular set of restraints and conditions related to its charging and discharging regime. Many types of batteries require specific charge controllers therefore charge controller designed for one type of battery cannot be used with another type.

Efficiency of battery is the ratio of charges that enter the battery during charging compared to the number that can be extracted from the battery during discharging. Losses that reduce efficiency are primarily due to the loss in charge due to secondary reaction. Again, the efficiency depends from type of battery.

Battery lifetime for application that is regularly charged and discharged the most appropriate measure of lifetime is the number of charge/discharge cycles over which the battery maintains a given fraction of its capacity. Since the battery involve chemical reactions and the materials used in batteries are susceptible, the performance of battery goes down with the time. For the system with no frequent charge/discharges battery lifetime can be specific in years. Improper use of battery can greatly accelerate battery aging and decrease the number of cycles over which battery can be used [18].

The voltage of the battery is determined by chemical reactions in the battery, concentration of the battery components and the polarization of the battery. Each battery has nominal voltage specified.

There are 3 main types of batteries. used in the PV systems:

- Lead-acid battery
- Lithium Ion battery
- Redox Flow battery

Lead acid batteries

The oldest form of energy storage system. They have been common storage option for micro-grids or grid-independent electrical power systems. They have low cycle life ranging from 2000-2500, round-trip efficiency of 70-90% and lifespan of 5-15 years. They generally have a depth of discharge of around 60 %. This means that only 60 % of its capacity can be used. They are identified as low-cost battery technologies which is one of the reasons they widespread in renewable energy applications [20].

Lithium-Ion

They are widely used in smaller appliances, such as mobiles, laptops. They can discharge deeper and have a longer life-time than lead-acid batteries, around 80-90%. They will have about 4000-6000 cycles at 80% discharge, so they will have a lifespan of 13-18 years. The round-trip-efficiency is about 100 %. The main drawback of that they are about 50 % more expensive than lead-acid batteries for the same amount of storage [21].

Flow Batteries

One of the advantages is that flow batteries have 100 % depth of discharge, which means that the battery can be entirely discharged in the cycle with no negative effects on the lifespan of the battery. Round -trip efficiency is generally considered around 85%. They can tolerate extreme weather conditions up to 50 °C. Disadvantages is quite low lifespan comparing to lithium-ion batteries, which is 4000 at 100 % discharge. The price of flow batteries is quite high, around 20 % more than lithium -ion batteries [22].

3. Design and Analysis

3.1. Building location and area

The residential building which is chosen as a case study is located in Whitlawburn, the residential area of Cambuslang, which is a suburb town on south-eastern outskirts of Glasgow.

It is a multi-storey tower block composed from 12 floors. Specific flor Plan and elevations can be found in the Attachment 1. The floor surface of each floor is 620 m^2.

In general ground source heat exchanger can be installed anywhere where is a space free of buildings such as parking's, streets, green spaces in the nearest area of the building. Considered location have quite a lot of space around the tower block. 2 locations were chosen as a potential spot for the ground exchanger and marked on the map with green and purple colour (Figure 17)

Considered building has around 620 m^2 of roof space. Figure 17 shows potential location for a PV system marked on the map using red colour.

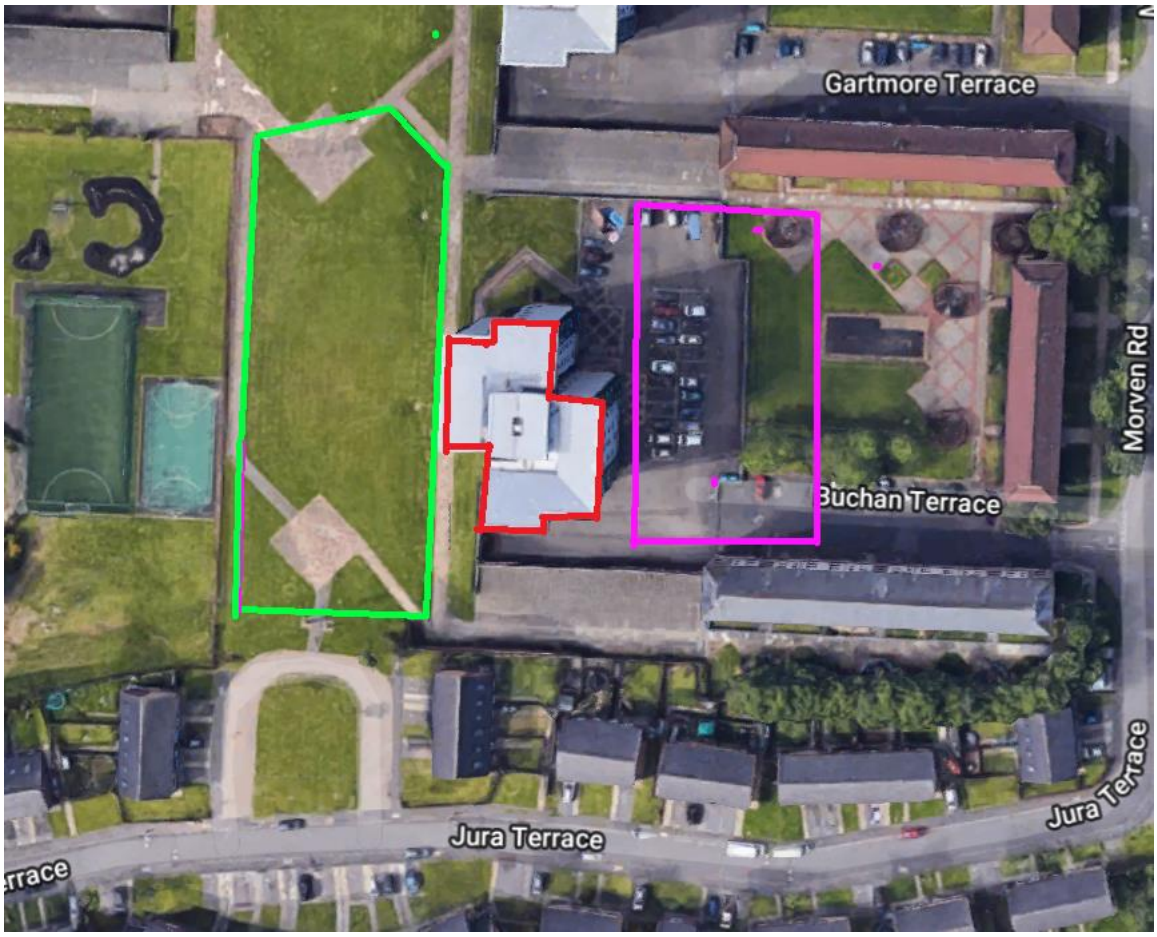

Figure 17 Map showing potential location of GHE and PV system

3.2. Selection of the Technology and Schematic of the System

Considering the specific of the building for residential purposes and the type of heating in the building, which is water heating, brine-to-water heat pump was chosen as a main heating and hot

water supply device in the building. The system has integrated thermal storage for load balancing purposes and reducing peak demand.

Due to high heating loads required caused by the fact it is a multifamily building ground-coupled system was chosen with vertical borehole heat exchanger. This type of system allows for more efficient heating related to stable ground temperatures and less ground space needed for situating required length of the heat exchanger. It is also most common type of system used for bigger applications.

The PV system is chosen to be composed from polycrystalline modules due to relatively high efficiency and affordable price. The system is grid connected and assisted with battery bank to allow store and use all produce output on the side. Lead-acid deep cycle batteries was chosen due to large size of the system and lowest cost from all available technologies.

Main components of the system are shown on the Figure 18. Heat at low temperature is extracted via borehole heat exchanger sized to match the evaporation power of the heat pump. The system has integrated thermal storage for load balancing purposes and reducing peak demand. PV array is mounted on the roof of the building. The system is grid connected to deliver energy load to heat pump while the output from the array is not sufficient. Additionally, there is a battery storage to maximise reduction of the electricity load taken from the grid.

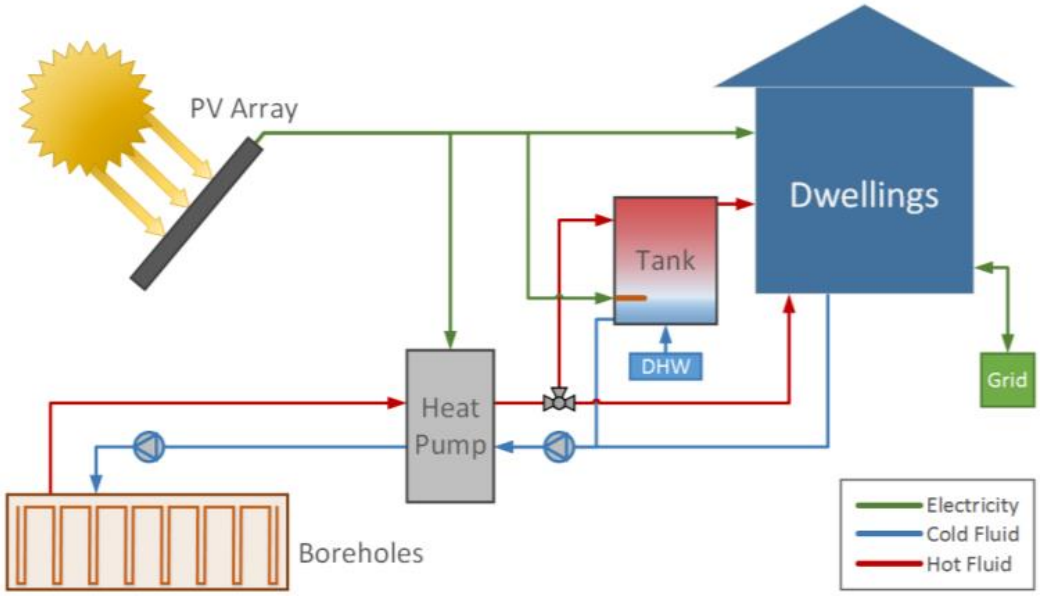

Figure 18 System Schematic [76]

3.3. Heating and DHW loads

3.3.1. Heating from ESP-r simulation

ESP-r software can was used for required heating load calculations. It is an energy performance simulation tool based on a finite volume, conservation approach in which a problem specified in terms of geometry, construction, operation, leakage, distribution etc. is transformed into a set of conservation equations which are then integrated at successive time-steps in response to stochastic climate, occupant and control system influences [23]. The simulation timestep can be adjusted between a fraction of a minute to an hour, as required.

To obtain heating load profile one floor of building with 49 thermal zones was modelled and the simulation performed for the time step of 1 hour. Resulted heating load was scaled up to generate the load for entire building by multiplying it by number of floors.

Geometry of single floor of the building have been replicated according to floor plan (Appendix 1). Obtained model shown on Figure 19. Weather file from Dundee was used as the reference climate data. Annual ambient temperature profile shown on the Figure 20. The Construction of the model have been updated according to U- values taken from the previous study, the values summarised in the Table 2. For the heating control the set point during the night and day was chosen. Operation parameters for the thermal zones was adjusted according to available design standards and Esp-r patterns. All operational parameters values used summarised in the Table 3.

Table 2 U-values for a tower block at West Whitlawburn

Section	**U-value**
External Walls	0.27
Floor	0.7
Windows	2.0

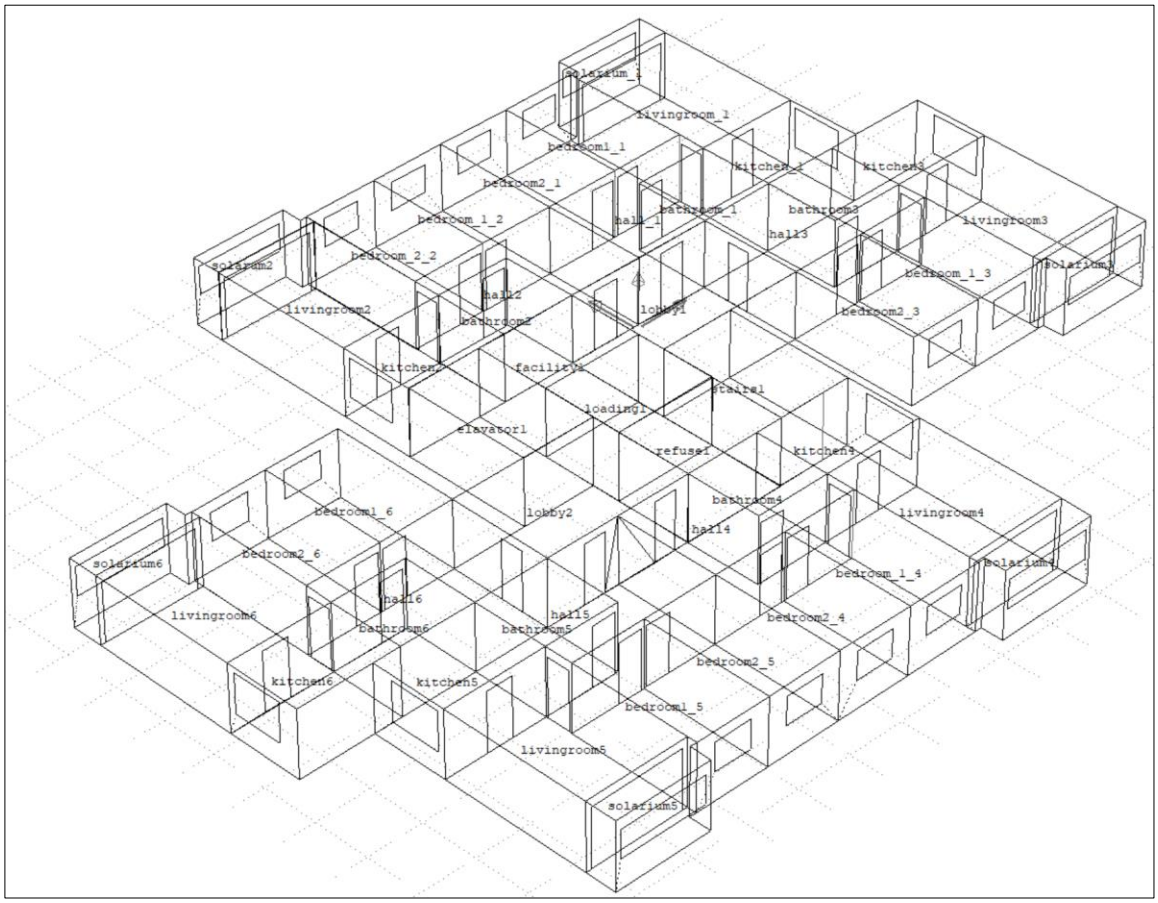

Figure 19 Model geometry in ESP-r with 49 thermal zones defined

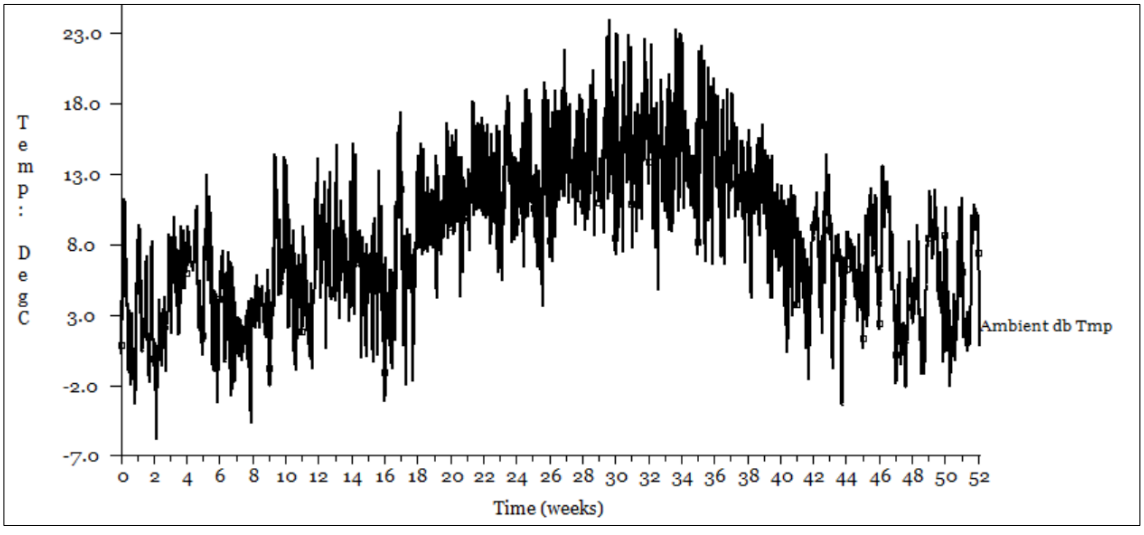

Figure 20 Annual ambient temperature profile

Table 3 Control and Operation parameters for the model

Control			
Heating set point			
	0-7h	off °C	
	7-24h	20 °C	
Summer	7-24h	18 °C	
Operation			
Infiltration-natural ventilation	All rooms	0.55 ac/hour	
Ventilation	Bathroom	3 ac/hour	
Casual gains	Bedroom	5.5 W/m^2	All weeks 0-24h
	Livingroom	14.5 W/m^2	Weekdays, Saturdays 8-20 h
	Kitchen	142.8 W/m^2	Weekdays, Saturdays 10-23h
	Lobby	6.7 W/m^2	Weekdays 9-18

Simulation was run for intervals of 15 minutes. Obtained annual space heating load displayed on Figure 21

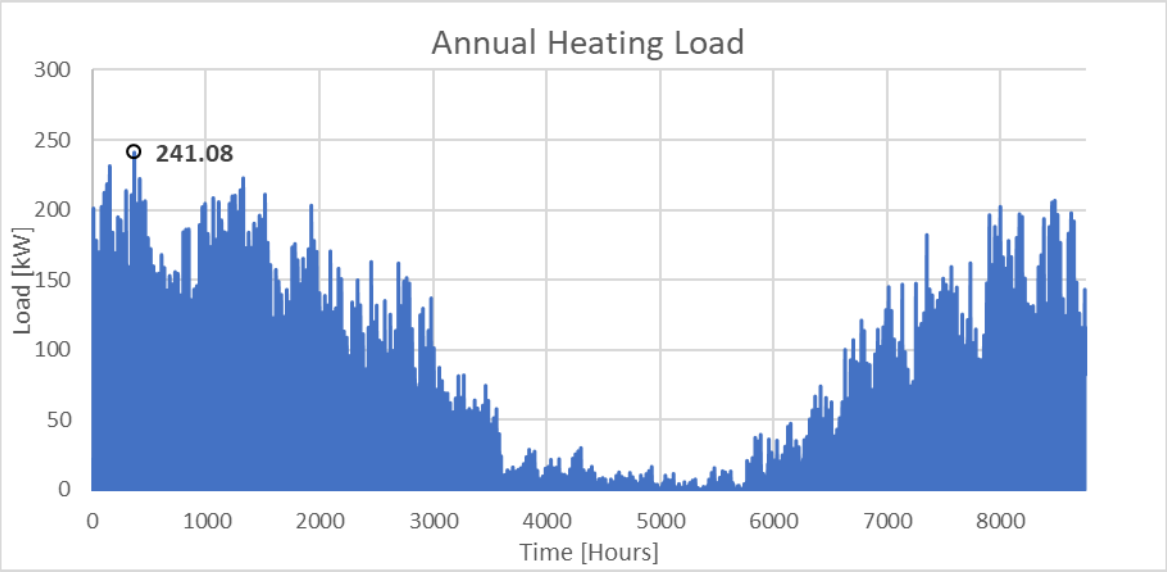

Figure 21 Annual heating load profile

3.3.2. Domestic Hot Water Load

Domestic Hot Water profile can be calculated using software DWHcalc 2.20b program. According to the documentation [24] there are 4 categories of loads considered: A: short load (washing hands etc), B: medium load (dish-washer etc.) C: bath: shower

For each category mean flow rate is defined. Each category profile is generated separately and superposed afterwards. The values of the flow rates are spread around mean value with a gaussian distribution:

$$prob(\dot{V}) = \frac{1}{\sqrt{2*\pi*\sigma}} exp \frac{-(\dot{V}-\dot{V}_{mean})^2}{2\sigma^2}$$

A probability function describes variation of the load profile during the year. calculated as the product of daily, weekly, seasonal probability distributions and the holiday step functions for every time step:

$$p(t) = p_{day}(t) * p_{weekday}(t) * p_{season}(t) * p_{holiday}(t)$$

$p_{day}(t)$ −Superposition of the Gaussian function as show on the Figure 4

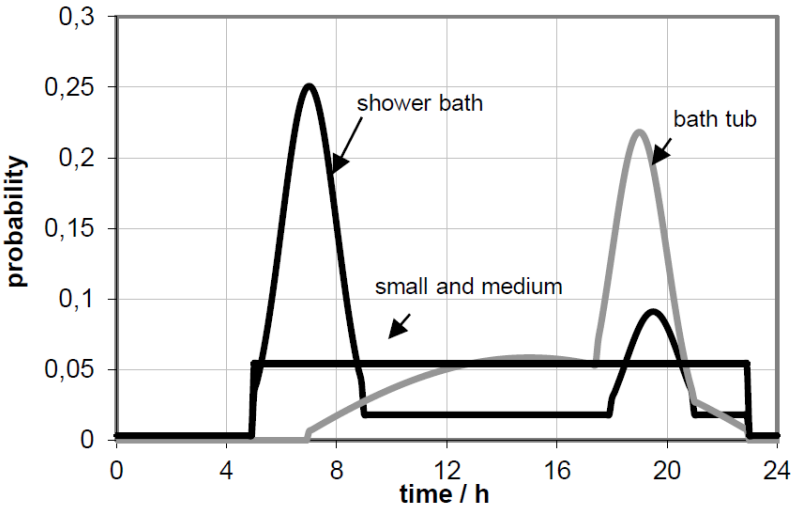

Figure 22 Probability Distribution load during the day [24]

$p_{weekday}(t)$- is a function to take different mean draw-off volumes on weekdays compared to weekend-days e.g. for 120%:

$$p_{weekdays} = \begin{cases} 0.95 for\ t \in week\ days \\ 1.15 t \in weekend - days \end{cases}$$

$p_{season}(t)$-seasonal variation described by sine function with a period of 356 days as on the Figure 5

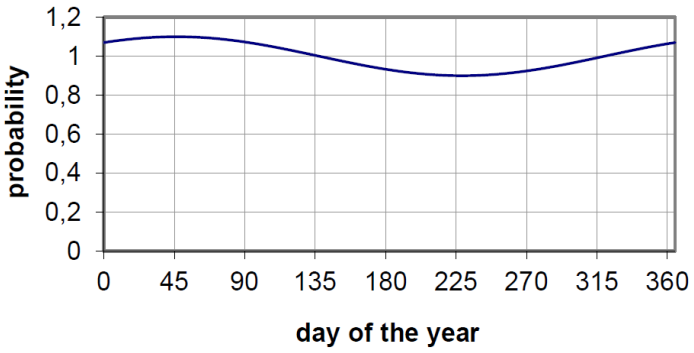

Figure 23 Sine function describing seasonal probability variations [24]

$p_{holiday}(t)$- considers reduced hot water consumption during a holiday period. For multi-family houses it's a period of 2 months within which holidays are considered for each household in the building. Duration of holiday period per household and consumption rate are to be specified. Start date of each single holiday period is randomly generated.

The cumulative frequency method is used to distribute draw-off incidences among the year according to probability function. Probability function in then integrated over the year and normalized

$$I(t) = \int_{tmin}^{t} p(t)dt$$

Afterwards the number of draw-offs during the year is calculated. The same number of random values between 0 and 1 is generated and assigned to a flow rate in the order of occurrence.

Typical values for calculations of domestic hot water usage are taken from the BSI standard. Design hot water usage value for the simple residential is 25-60 l/day [25]. The number of occupants is assumed to be one more than the number of bedrooms in each flat. Based on that total draw-off volume of the multi-family house can be calculated as:

$$V_{w,day} = N_F * N_H * n * v_{w,day} = 12960 \frac{l}{day}$$

Where:

$V_{W,day}$ – Total daily requirement for hot water in the tower block,N_F – number of floors in the building, N_H – number of flats on each floor, $n - number\ of\ occupants$, $v_{w,day}$ – hot water demand per person

Table 4 Input parameters for DWH load calculations

Main Window				
House type	Multifamily house			
No. of households	72			
No. of categories	4			
Time step duration	15 mins			
Total duration	365 days			
Total mean daily draw off volume	12960			
Probability Distribution Window				
Probability during the day	DHW standard distributions			
Probability weekend-day/weekday	120%			
Probability seasonal variations	Sine function: amplitude of sine: 10 %, sin max:45 day of the year			
Holiday period consumption	0%			
Multifamily house starts and end period	1/7-1/09			
Number of holidays during the period per household	14			
Flow Windows				
Draw off-features	Cat1	Cat2	Cat3	Cat4
Mean flow rate per draw-off	60l/h	360l/h	840l/h	480l/h
Draw-off duration	1min	1min	10min	5min
portion	14%	36%	10%	40%
Standard deviation	120l/h	120l/h	12l/h	24l/h
Min. flow rate	1 l/h			
Max. flow rate	1200 l/h			

Results from simulation for multi-family house with 72 flats returned the load profile of hot water for all year in l/hour. The data was then converted to kW using the following formula:

$$Q_{DWH} = \frac{\dot{V_{DWH}} \rho c_p \Delta t}{3600}$$

Where:V_{DWH} −volume floe rate of the hot water, $\rho = 1000 kg/m^3 -$ specific volume, $c_p = 4.2 \frac{kJ}{kg*K}$ −specific heat of water

Obtained heat load for DHW displayed on the Figure 24 and aggregated DHW with space heating on the Figure 25.

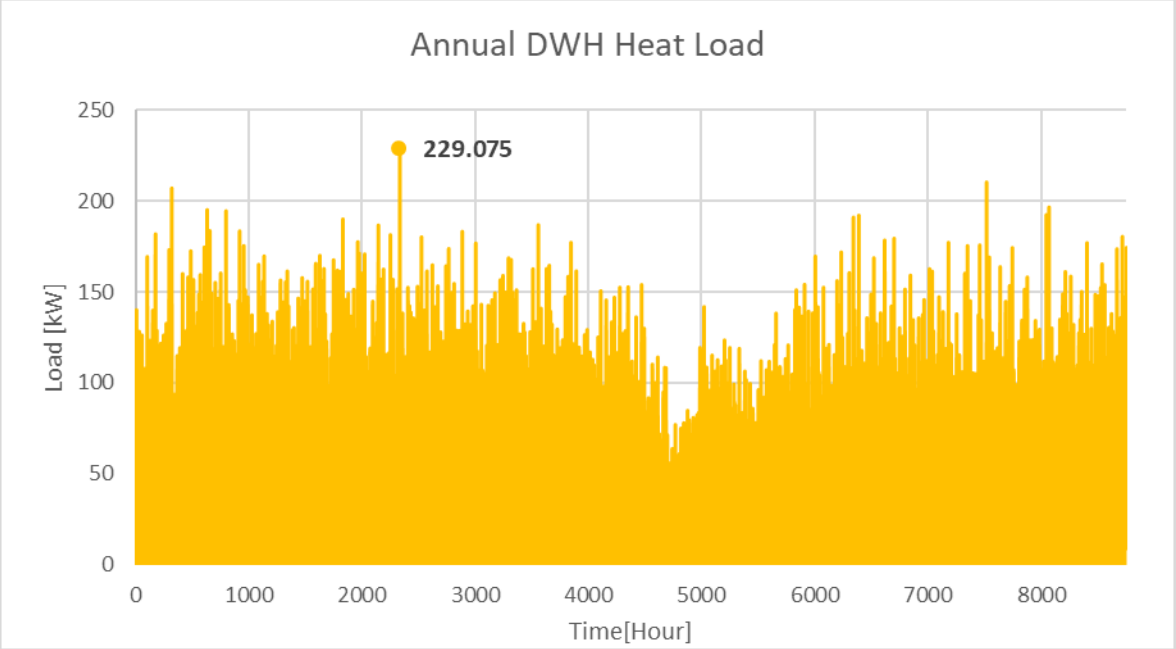

Figure 24 Annual DWH heat load

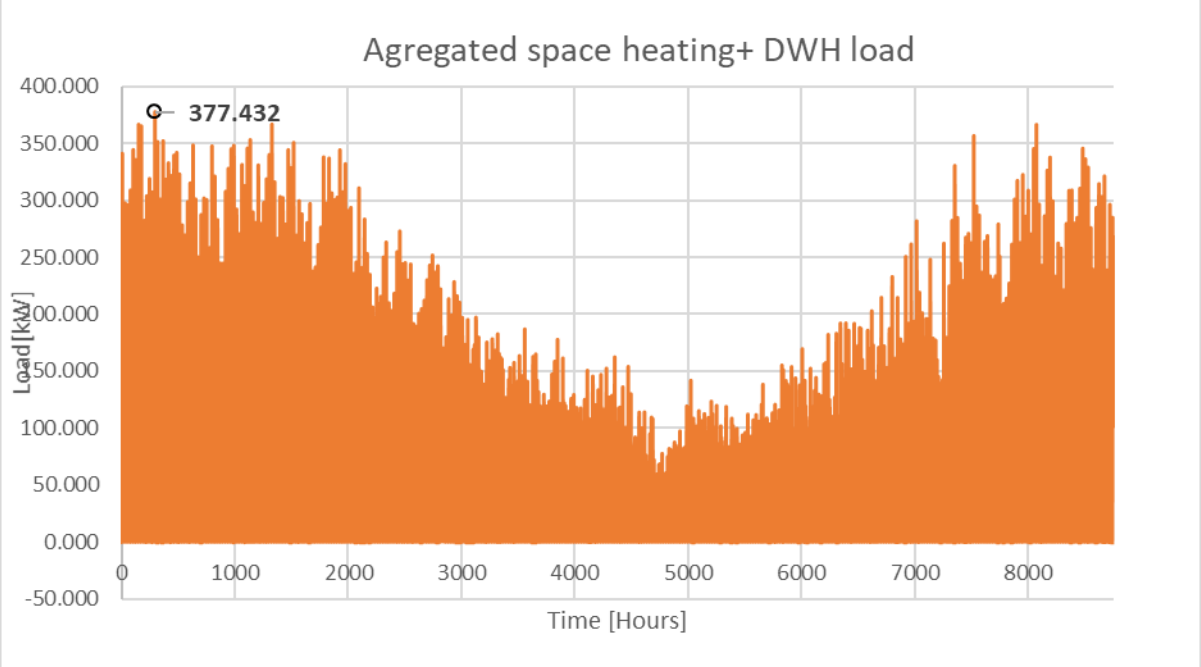

Figure 25 Aggregated space heating + DHW

Peak heating load occurred in January and have value of 241.05 kW while DHW peak load was 229.075 kW. Aggregated peak occurred peak load was 377.432 kW. Total energy demand per year is $E_{dem,a} = 617880$ kWh.

3.4. Thermal Store and Heat Pump

3.4.1. Thermal Store

Custom sizing methodology based on the research paper was used to calculate optimal storage size for the diurnal shift period [9]. Thermal storage is used to reduce heat source capacity for peak load and allows for scheduled operation of the heat pump. Based on the heat demand trend in the coldest day shown in Figure 26. The time of 3 peak hours was chosen to be supported by storage. Calculation performed in Excel spreadsheet with use of previously generated load profiles.

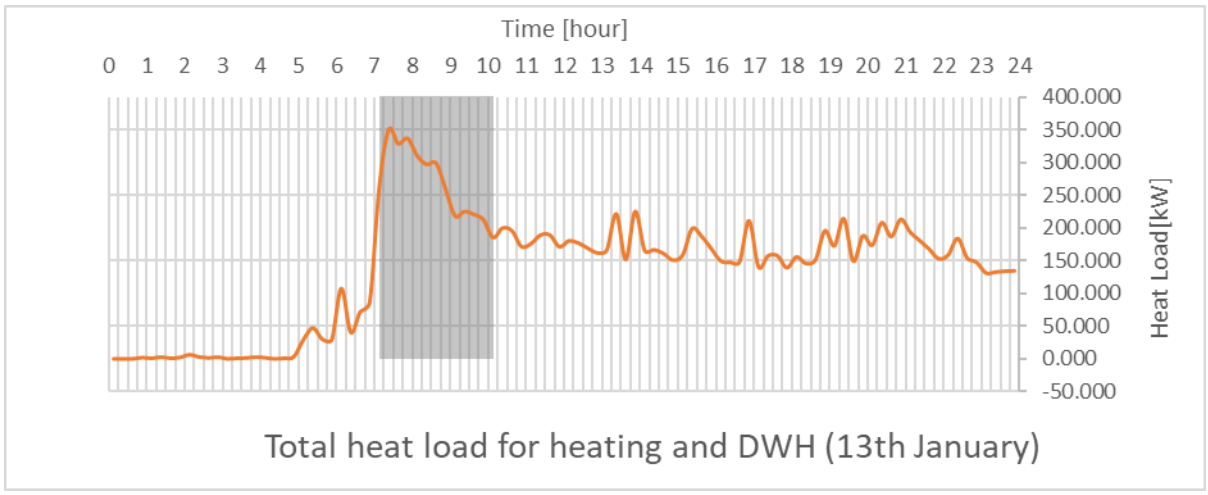

Figure 26 Heating load for the coldest day in a year

Number of segments for desired daily load shift was calculated as:

$$n_{seg} = 365 * \frac{24}{3} = 2920$$

Energy balance was enforced for each time to determine amount of energy the store would need to supply during each segment.

$$\frac{dP_{tes}(t)}{dt} = P_{gen}(t) - P_{dem}(t) - P_{losses}(t)$$

Where:

$P_{gen} -$ *heat input to the store*

$P_{dem} -$ *thermal demand on the store*

$P_{losses} -$ *energy losses from the store*

For the profiles generated from the simulations:

$$\frac{P_{tes}[k+1] - P_{tes}[k]}{ts} = P_{gen}[k] - P_{dem}[k] - P_{losses}[k]$$

k- k-th time step of the simulation.

Thermal storage is designed to cover peak morning load. For the storage sizing calculations, the heat input to the store is assumed to be 200 kW – power output from the heat pump.

$P_{gen}\,[k] = 200\ kW$

$E_{tes}[k] - E_{tes}[k+1] = E_{dem}[k] + E_{losses}[k] - E_{gen}[k]$

Energy required in the store:

$Q_{tes}[k] = E_{tes}[k] - E_{tes}[k+1] = E_{dem}[k] + E_{losses}[k] - E_{gen}[k]$

Required size for each q-th time segment is the sum of all elements in the segment:

$$Q_{tes,q}[k] = \sum_{k=1}^{nts,seg} E_{dem}[k] + \sum_{k=1}^{nts,seg} E_{losses}[k] - \sum_{k=1}^{nts,seg} E_{gen}[k]$$

Storage capacity is the function of the losses at each time step so required size of store for each q-th with no losses were calculated first (perfectly insulated thermal store).

$$Q *_{tes,q}[k] = \sum_{k=1}^{nts,seg} E_{dem}[k] - \sum_{k=1}^{nts,seg} E_{gen}[k]$$

Heat loss was assumed as a worst-case loss rate of around 1kWh/day.

$$E_{losses,24h} = 1\ kWh$$

The losses at each time segment is related to number of hours per segment and rate of energy loses per day:

$$\sum_{k=1}^{nts,seg} E_{losses}[k] = E_{losses,24h} * \frac{n_{h,segment}}{24}$$

$$Q_{tes,q}[k] = \left(\sum_{k=1}^{nts,seg} E_{dem}[k] + E_{losses,24h} * \frac{n_{h,segment}}{24} - \sum_{k=1}^{nts,seg} E_{gen}[k] \right)$$

To determine the maximum required storage capacity the max value from all time segments needs to be taken:

$$Q_{tes} = \max\left(Q_{tes,q}\right) q = 1, \dots\dots, 2190$$

The storage volume can be calculated as follows:

$$V_{tes,q} = \frac{3600 * Q_{tes,q}}{\rho c \Delta T}$$

Table 5 Results from the Thermal Storage sizing Algorithm

n_{seg}	2920	-
$n_{ts,seg}$	12	-
$\sum_{k=1}^{nts,seg} E_{dem}[k]$	703.229	[kWh]
$\sum_{k=1}^{nts,seg} E_{losses}[k]$	0.125	[kWh]
$\sum_{k=1}^{nts,seg} E_{gen}[k]$	600 (3*200)	[kWh]
Q_{tes}	103.283	[kWh]
$V_{tes,q}$	4.448	$[m^3]$

The storage with volume 5000 l was chosen, the details in the Table below:

Table 6 Thermal Storage details [26]

Volume	5000 l
Total Height	2790 mm
Diameter	1600mm
Parts	1 heat exchanger

3.4.2. Heat Pump

Heat capacity of the heat pump considering the daily load and use of thermal storage is chosen to be 240 kW. Specification of the device summarised in the Table 7

Table 7 Heat pump specification

Rated heating output Q	240 kW
Power Consumption W_{comp}	50.4 kW
COP in heating mode	4.76
Max Flow temp	60°C
Brine Temp	5°C

$COP_{h,Carrnot}$	6.05
System efficiency	0.786
Refrigerant	R410A

Performance characteristic:

The characteristic was generated using the formula:

$$COP_{HP} = \eta_s * COP_{h,carnot} = 0.79 * \frac{T_c}{T_c - T_e}$$

Impute temperature parameters summarised in the Table 8.

Table 8 Input parameters for the COP characteristic

Tc	Te	COP 65	COP 60	COP 55	COP 50	COP 45	COP 40
65	0	4.087	4.362	4.687	5.078	5.554	6.150
60	1	4.151	4.436	4.774	5.181	5.681	6.308
55	2	4.217	4.513	4.864	5.289	5.813	6.474
50	3	4.285	4.592	4.958	5.402	5.951	6.649
45	4	4.355	4.674	5.055	5.519	6.096	6.834
40	5	4.428	4.759	5.156	5.642	6.249	7.029

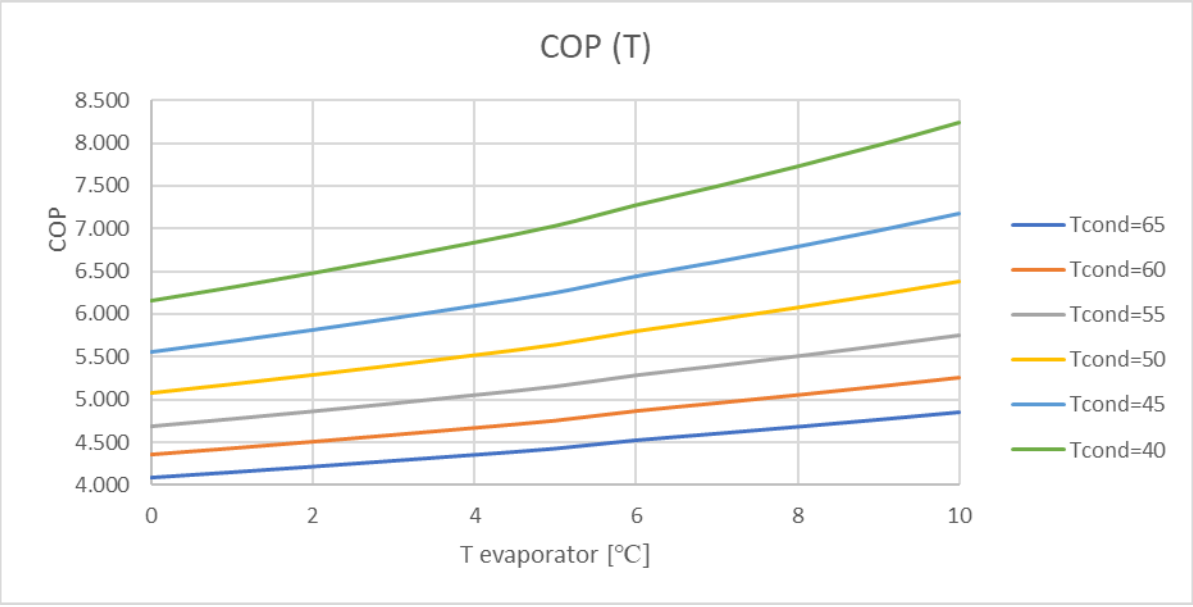

Figure 27 Performance of the heat pump for different temperatures in condenser and evaporator

Efficiency of heat pump depends of the temperature difference between the condenser and evaporator. Figure 27 shows the influence of the temperature difference on the COP value of chosen heat pump. There is an increase of COP with increasing temperature in evaporator as well as increase of COP with decreasing temperature in condenser. The temperature in the evaporator and condenser depends from the outlet temperatures of heat exchanger fluid and the temperature from the heating installation. Carnot COP is the max theoretical efficiency of the heat pump. Real systems have always lower efficiency caused mainly by irreversibility of the processes.

3.5. Borehole heat exchanger

Required length of the borehole heat exchanger can be calculated as:

$$L_i = \frac{q_{h,i} * R_b + q_{pm,i} * R_{pm,i} + q_{cm,i*} R_{cm} + q_{h,i} * R_{h,i}}{(T_m - (T_g + T_{p,i})}$$

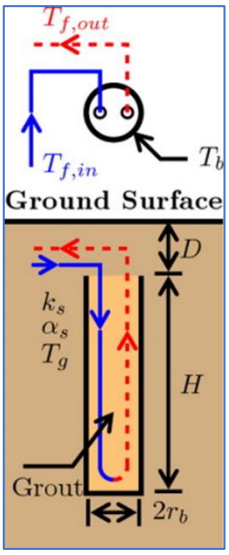

Figure 28 Borehole geometry

3.5.1. Ground loads

Ground loads components are calculated as the heat required to be delivered to the heat pump evaporator. System is being designed with usage of thermal storage to reduce the heat pump capacity therefore the max possible ground load is calculated for the max designed power output from the heat pump, not for the max heat demand.

$$q_{cm,i} = Q_{mean,i} * \frac{1}{COP^{HP}}$$

$$\bar{q}_{pm,i} = \frac{\sum q_{pm}}{ni}, q_{pm,i} = 0 \; for \; i = 1$$

$$q_{h,i} = Q_{peak,i} * \left(1 - \frac{1}{COP^{HP}}\right)$$

$$Q_{peak,i} = \begin{cases} Q_{max}\ if\ Q_{max} < P_{HP} \\ Q_{HP}\ \ if\ \ Q_{max} \geq P_{HP} \end{cases}$$

Where:

COP^{HP} −Coefficient of Performance for the heat pump, $P_{mean,i}$ − Mean heat load in the month, $\frac{\sum q_{pm}}{ni}$ −avarage ground load for preceding months, $P_{peak,i}$ − peak heat load to be covered by heat pump , P_{max} − peak heat load , P_{HP} − max designed power output from the HP.

3.5.2. Equivalent ground thermal resistances

Effective ground thermal resistances are calculated for their step duration.

$$R_{pm,i} = \frac{G\left(Fo_{th,i-0}\right) - G(Fo_{th,i-tpm,i})}{\lambda_g}$$

$$R_{cm,i} = \frac{G\left(Fo_{th,i-tpm,i}\right) - G(Fo_{th,i-tcm,i})}{\lambda_g}$$

$$R_{h,i} = \frac{G(Fo_{th,i-tcm,i})}{\lambda_g}$$

$$Fo = \frac{4\alpha t}{d\text{^}2}$$

Where:

Fo −Fourier Number, d − borehole diameter, α − thermal diffusivity of the soil, t −the period characterizing the impulse

G factor is based on the theory of the cylindrical source. And can be obtained by:

$$G = 0.0758 * \ln(Fo) + 0.1009 \text{ for Fo} > 2$$

Borehole thermal interference is evaluated at the end of each month using the concept of thermal penalty

$$T_p = \frac{q_i}{2\pi\lambda_{g*}L} * [g_{n,i} - g_{1,i}]$$

q_i- average ground load up to that point (from all previous months), L- Required borehole length

λ_g- ground conductivity

$[g_{n,i} - g_{1,i}]$- g functions generated for specific D, rb, H, nb and B of the borehole, for the

G-functions varies according to the nondimensional time t/t_s where:

$$t_s = \frac{H^2}{9\lambda_g}$$

H −Borehole height

Python script was used for calculating g-functions using a boundary condition of uniform and equal heat extraction rate for all boreholes, constant in time [27]. Figure 29 shows an example of generated function verified against the g-functions presented by Cimino and Bernier [28].

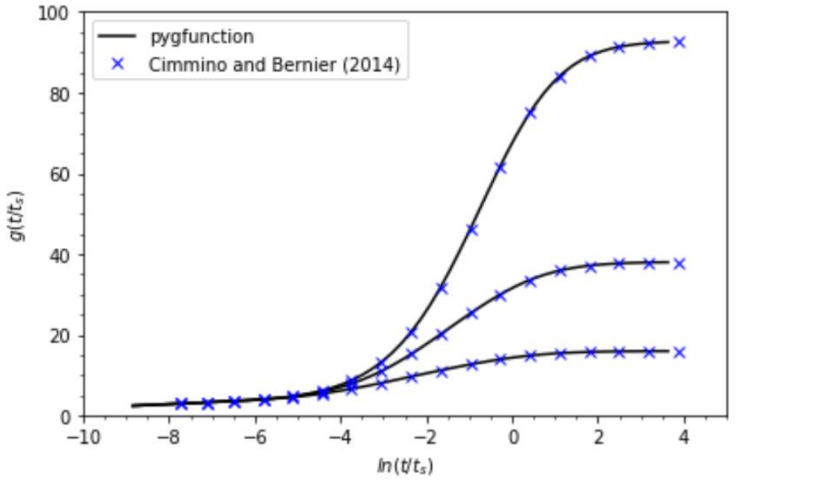

Figure 29 G-functions of rectangular fields of 3 x 2, 6 x 4 and 10 x 10 and borehole dimensions: D=4.0; H= 150.0; rb=0.075;B=7. [13]

3.5.3. Required borehole length

Calculation of the required bore field length requires iterative process as the temperature penalty depends on the borehole height which is unknown at the start of the calculations and an assumption needs to be taken. The flown chart describing the process shown on the Figure 30. Iteration was performed in the Excel spreadsheet. All used formulas were validated by manual calculations.

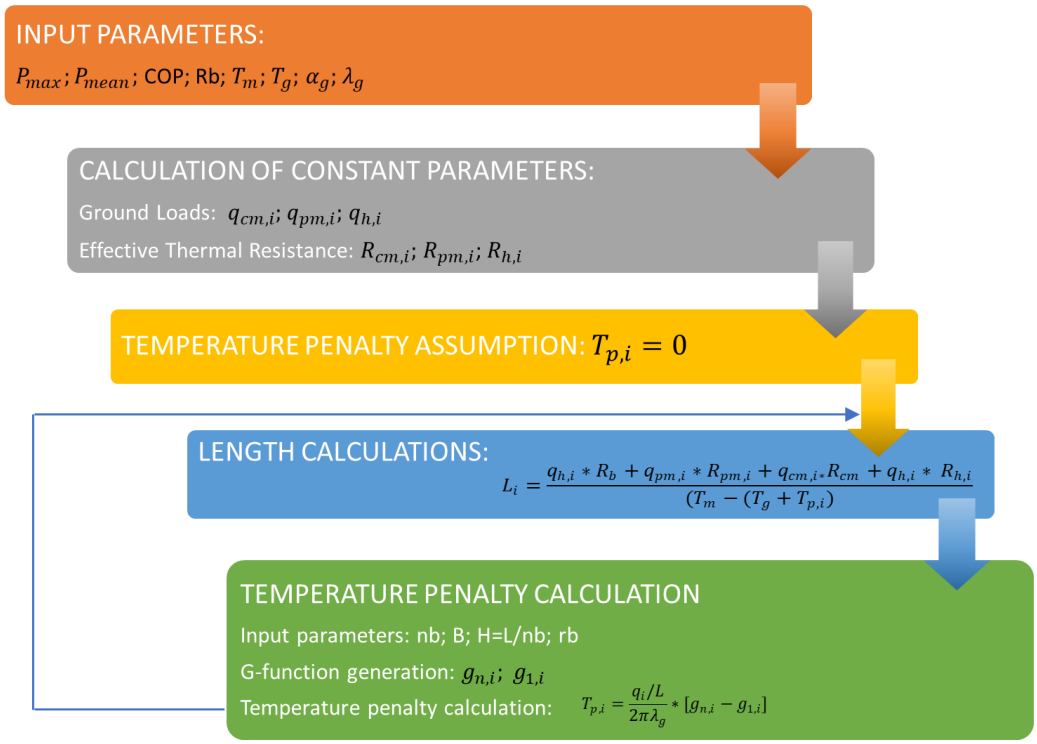

Figure 30 Flow chart of iterative process of sizing GHX

Input parameters and assumptions

In presented methodology it is assumed that year is composed from 12 months each with 30.42 days for a total of 365 days. The number of hours with peak load for each month is assumed and based on the max hourly load rate. The temperature penalty is calculated with use of the g-functions generated for each bore field parameters.

Month when the system is to be started is January. Monthly ground loads need to be ordered starting from the first month of operation. Input parameters for the calculations summarised in the Table 9 below.

Iteration process start from the following assumption:

$$T_p = 0$$

And calculations should be repeated until following condition returns True.

$ABS(L_{new} - L_{old}) * 100\% < 1\%$

Table 9 Ground and borehole input parameters

Ground conductivity	λ_g	2.25 W/mK
Ground diffusivity	α_g	0.075m^2/day
Ground Temperature	T_g	10 ℃
Heat pump rated power	Q_{HP}	240 kW
Coefficient of performance	COP_{HP}	4.76
Number of boreholes	nb	64
Pattern		8x8
Borehole thermal resistance	R_b	0.1 mK/W
Borehole radius	rb	0.075 m
Borehole spacing	B	7.5m
Borehole buried depth	D	4m
Mean fluid temperature in the heat exchanger	T_m	0 ℃

As we can see from the results in the Table 10, max. length of exchanger of 5807 m is required for the February while the min. value of 2356 was obtained for August. Required length of the heat exchanger for each month is proportional to the average ground load for that month as indicated on the Figure 31. The Details of ground heat exchanger, sized according to the rule for the worst ground conditions, summarized in the Table 11.

Table 10 Equivalent thermal resistances, Ground loads, corresponding Length and Temperature penalty at each month for Heating

Month	qpmi [kW]	qcm,I [kW]	qh,I [kW]	Rpm,I [mK/W]	Rcm,I [mK/W]	Rh,I [mK/W]	L [m]	Tp [K]
Jan	0	90460	189580	0.000	0.162	0.093	5763	-1.11
Feb	90460	87660	189580	0.023	0.171	0.076	5677	-1.11
Mar	89060	75507	189580	0.037	0.215	0.033	5047	-1.16
Apr	84542	58722	181720	0.047	0.232	0.015	4360	-1.17
May	78087	45986	144578	0.054	0.175	0.072	4153	-1.06
June	71667	28426	104506	0.060	0.185	0.062	3007	-1.18
July	64460	18632	96166	0.066	0.199	0.048	2515	-1.17
Aug	57913	20770	79405	0.070	0.185	0.062	2356	-1.18
Sep	53270	32780	122867	0.074	0.245	0.002	2753	-1.11
Oct	50994	54000	173982	0.078	0.232	0.015	4026	-0.92
Nov	51294	69252	189580	0.081	0.180	0.067	5254	-0.80
Dec	52927	82349	189580	0.084	0.158	0.089	5807	-0.82

Table 11 Details of the design borehole heat exchanger

Total required length	5807
Bore field pattern:	8x8
Number of boreholes	64
Single borehole length	91
Borehole diameter	0.15m
Borehole spacing	7.5m

.

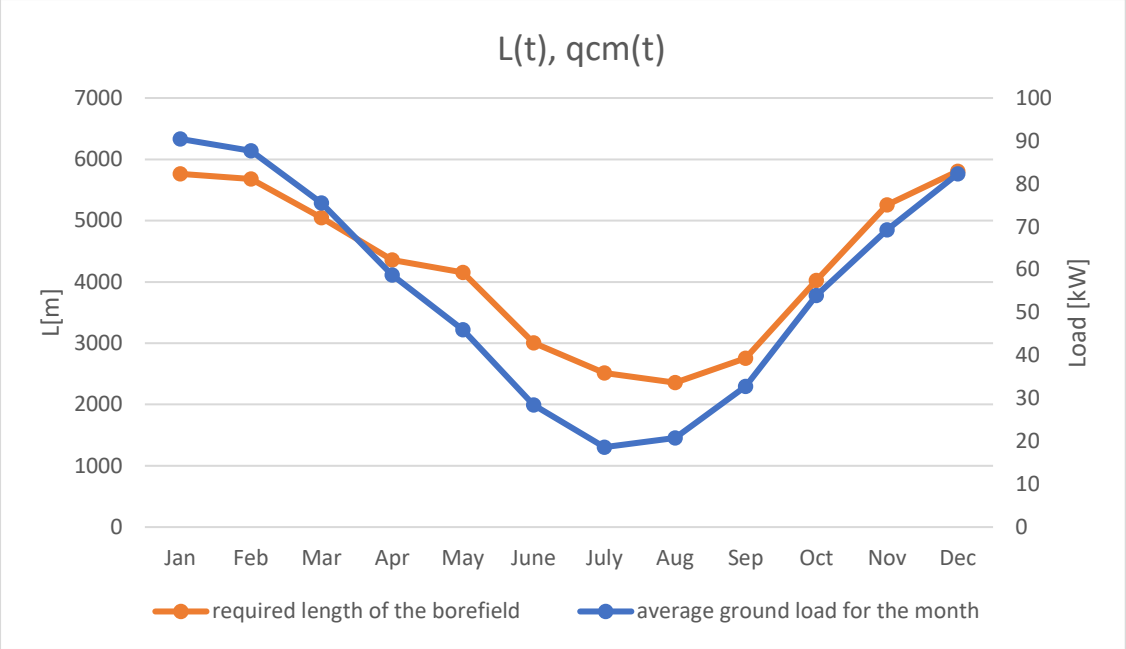

Figure 31 Length of heat exchanger compared to the mean ground load

3.6. PV installation

3.6.1. System Schematic

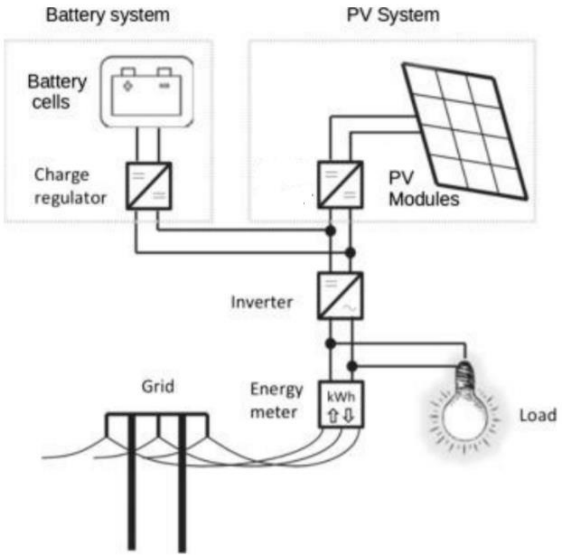

Figure 32 PV System schematic [29]

Heat pump is designed as the only source of heat in the building. Monthly diurnal energy consumption for the heat pump estimated from the demand profile:

$$E_{HP,m} = \sum_{i=1}^{720} \frac{Q_{d,i}}{COP^{HP}}$$

Required energy delivered to the heat pump to supply heat was calculated and the results displayed on the Figure 33 for every month of the year. Total annual required energy:

$$E_{HP,a} = 129816 \text{ kWh}$$

.

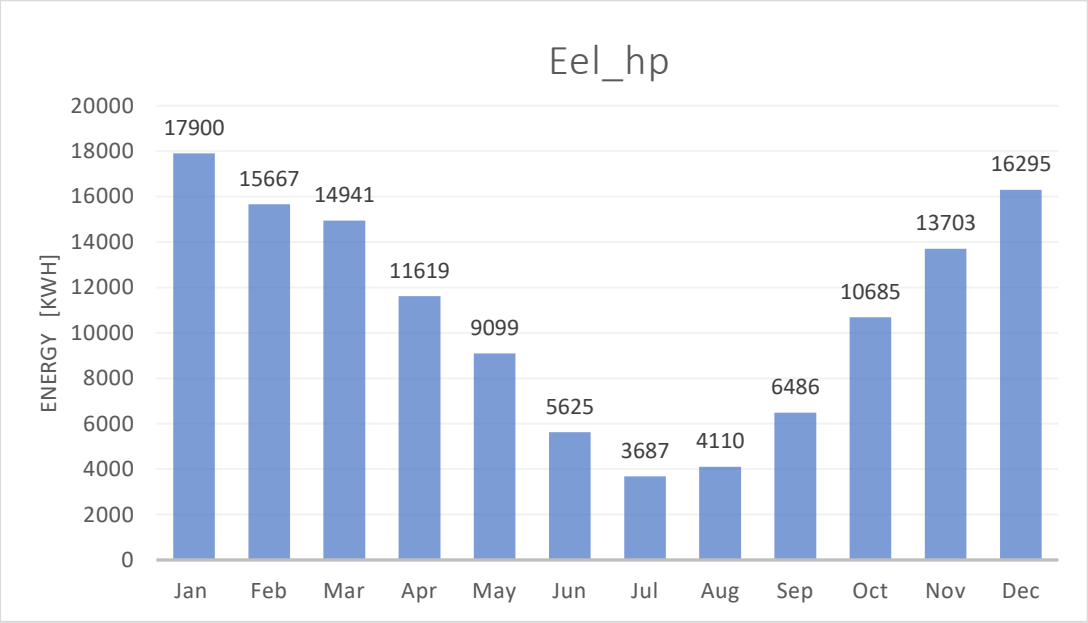

Figure 33 Heat Pump energy load through the year

3.6.2. Sizing the required PV modules:

Estimation of power generated from a solar module is done with a simple equation that uses the standard test conditions (STC) and normal operating cell temperature (NOCT) provided by manufacturer [30]. Solar model efficiency is represented by:

$$\eta_{pv} = \eta_{STC}(1 - \beta_P(T_c - T_{STC}) + \gamma log I_{tot})$$

Where:

η_{STC} −solar cell efficiency in STC

T_c −solar cell temperature

β_P −solar cell temperature coefficient

G − solar irradiance

γ −irradiance coefficient. $\gamma = 0$

The solar cell temperature can be estimated with equation:

$$T_c = T_a + (T_{NOCT} - 20℃)\frac{I_{tot}}{800W/m^2}$$

T_{NOCT} − nominal operating cell temperature

T_a −ambient temperature

3.6.3. Irradiance

Direct normal and diffuse radiation data on horizontal surface for those representative day of the month was taken from the weather data for Glasgow available on CIBSE website [31]. Direct horizontal irradiance can be calculated as:

$$I_{dh} = I_{dn} * sin\beta_s$$

3.6.4. Solar irradiation on the Inclined surface

Total radiation incident radiation on an exposed surface have 3 components: direct, surrounding-reflected and sky diffuse [32].

Direct irradiance formula: $I_{d\beta} = I_{dh} * \cos i_\beta / sin\beta_s$

Diffuse irradiance on same surface:

- Ground reflected: $I_{r\beta} = 0.5\left[1 - \cos(90 - \beta_f)\right](I_{dh} + I_{fh}) * rg$
- Sky component:

$$I_{s\beta} = I_{fh}\left(\frac{1+\cos(90-\beta f)}{2}\right)*\left(1+[1-\left(\frac{I_{fh}^2}{I_{gh}^2}\right)]sin^3\left(\frac{\beta_f}{2}\right)\right)*\left(1+\left[1-\left(\frac{I_{fh}^2}{I_{gh}^2}\right)\right]cos^2(i_\beta)sin^3(90-\beta_s)\right)$$

Angle of incidence is given by:

$$i_\beta = cos^{-1}(\sin\beta_s\cos(90-\beta_f)+\cos\beta_s cos\omega\sin(90-\beta_f)$$

Where:

$\omega = |\alpha_s - \alpha_f|$

I_{dh}, I_{fh} −dirrect and diffuse irradiance on the horizon surface, rg −ground reflectivity,

β_f, β_s − solar inclination and altitude respectively, α_s, α_f −solar azimuth and surface azimuth

$\alpha_s and\ \beta_s$ data for specific location and date was generated in online service [33].

3.6.5. Power output

Power output of solar module can be calculated as:

$$P_{pv} = \frac{G}{1000}P_{STC} * (1-\beta_P(T_C-25)$$

Energy capacity of one module can be than calculated per representative day in each month:

$$E_{pv,d} = \sum_{k=1}^{24} P_{pv}$$

Required number of panels to meet the heat pump demand for a day can be calculated as:

$$n_{pv} = \frac{E_{el,d}}{E_{pv,d}}$$

The number of panels is restricted by available roof space A_r. System placed on the flat roof requires 1m space from the edge of the roof and appropriate space between PV array rows to

avoid shading effect. The available roof space is 620 m2 and the panel area is 1.7m^2. From practical point of view the max number of units is assumed as:

$$n_{pv,max} = 150$$

Monthly Energy output from PV array can be calculated as:

$$E_{array,m} = \sum_{k=1}^{30} E_{pv,d,month} * n_{pv} * \eta_{inv}$$

Where:

$E_{pv,d,month}$ *−average daily energy output for specific month,* n_{pv} *−number of PV modules in array,* η_{inv} *−inverter efficiency*

3.6.6. PV Characteristic

To determine the availability of solar radiation on the inclined surface of PV module the irradiation for every hour of 21th day in each month was calculated. PV modules are assumed to face south (αf=180) with an inclination of 45 degrees to the horizontal surface (βf=45). Power output from module is a function of irradiation on inclined surface and the temperature of the cell. Power characteristic for a representative day of every month was calculated and results displayed on the Figure 34.

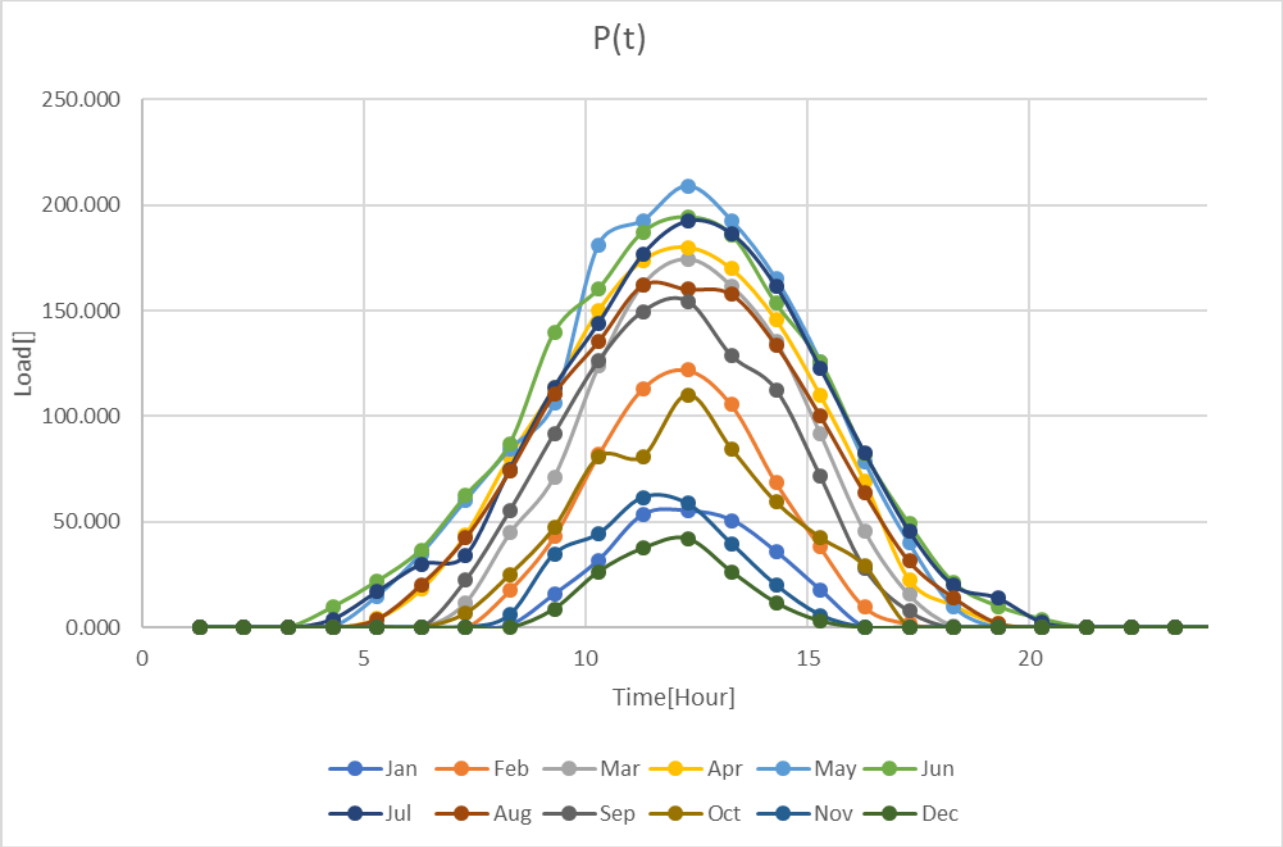

Figure 34 Power characteristic of the PV module with nominal power 235 W

Power load changes through the day according to solar radiation intensity. It can be noticed on the maximum power output according to characteristic can be achieved in May and the minimum power is expected to be generated in December. Characteristic shows as well how the power load from module changes during the day. Peak output at the afternoon around 12 when the irradiation is the most intensive. Chart shows as well how the output depends from the length of the day. On winter the module produces energy only for 6 hours per day while on summer the load is generated for approximately 15 hours per day.

From the resulted power load daily energy output was estimated for every month and summarised in the Table 12. That data will be used in the further chapters of annual electricity output from PV array.

3.6.7. Energy Output and Efficiency

Table 12 Estimated Energy output from 235W PV modules. Output for representative days of every month

Month	Latitude 55o51’ Longitude 4o15’ αf= 180o βf=45o [kWh]
January	0.262
February	0.602
March	1.040
April	1.295
May	1.494
June	1.532
July	1.423
August	1.213
September	0.949
October	0.566
November	0.271
December	0.157

Not only the irradiation affects the power capacity of PV module. Efficiency depends from the surface temperature of the cell. Figure 35, Figure 36 below show how the efficiency changes for the winter and summer day. Drop of the efficiency with the increase of the cell surface temperature is noticeable on both charts.

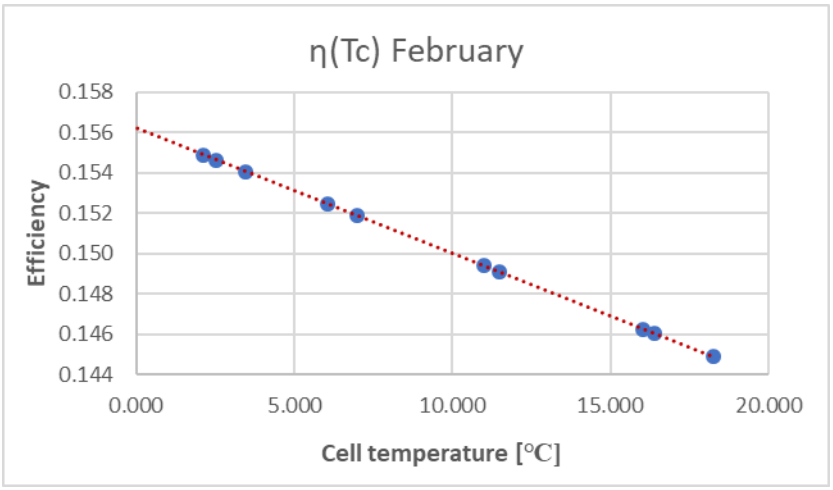

Figure 35 Cell temperature and efficiency on winter

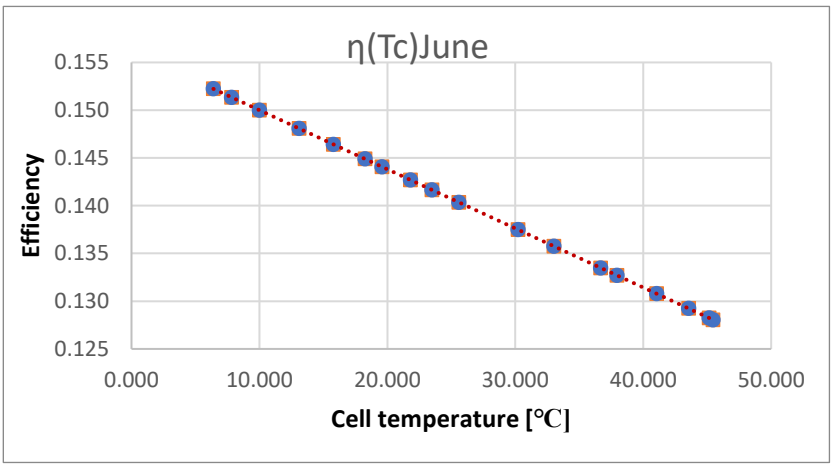

Figure 36 Cell temperature and efficiency on winter

Efficiency of module on winter can be higher than in summer as the outside temperature is lower, so as the surface temp of the module.

3.6.8. Sizing of the array

Design of the PV array was based on the worst case which is the maximum energy demand for a day. Required energy load profile (Figure 37) was generated for the winter day when the peak load appeared.

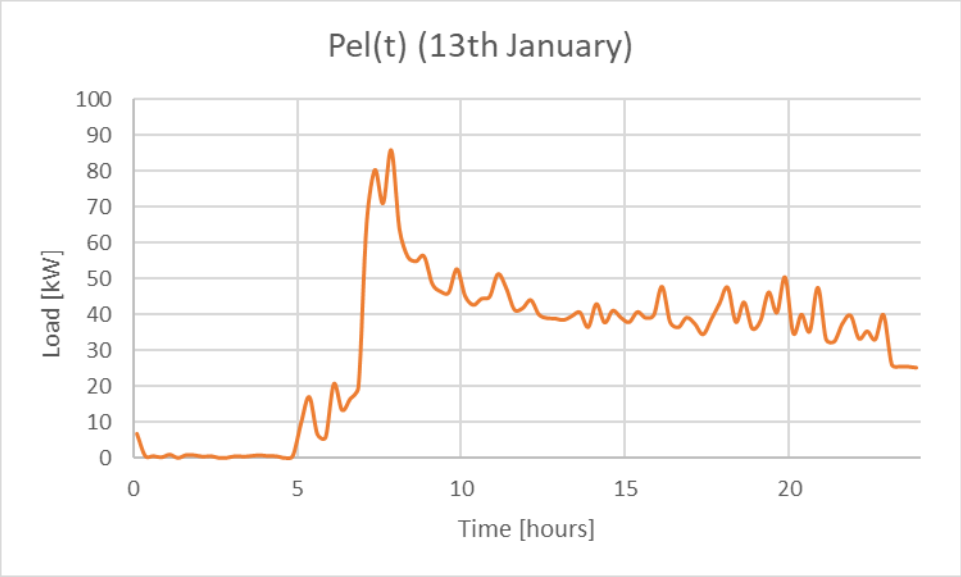

Figure 37 Electricity load profile of heat pump (13 th of January)

$E_{el,d} = 760.65\ kWh$

According to Table 9 One PV module can produce 0.267 kWh/day. Required array size can be then calculated as:

$n_{pv} = \frac{E_{el,d}}{E_{pv,d}} = \frac{760.65}{0.267} > n_{pvmax} \rightarrow$ The array will be composed from max number of panels assumed for the roof space: $n_{pv} = 150$.

Nominal installed power of PV array:

$$P_{n,array} = 235 * 150 = 35.25KW$$

It is not feasible to compose the system that will produce enough energy to meet the heat pump demand all year round. PV array composed from 150 modules was chosen.

3.6.9. Energy output and batteries required

Total Energy output from installed system for different months according to installed size of array and energy capacity illustrated on the Figure 38 and compared with the heat pump energy demand on the Figure 39.

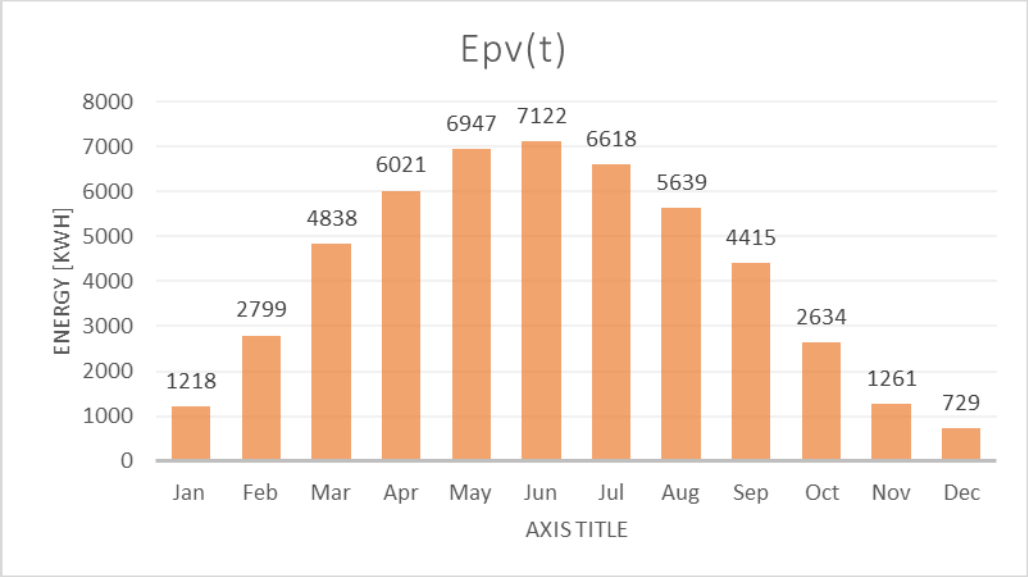

Figure 38 Monthly energy output from PV array

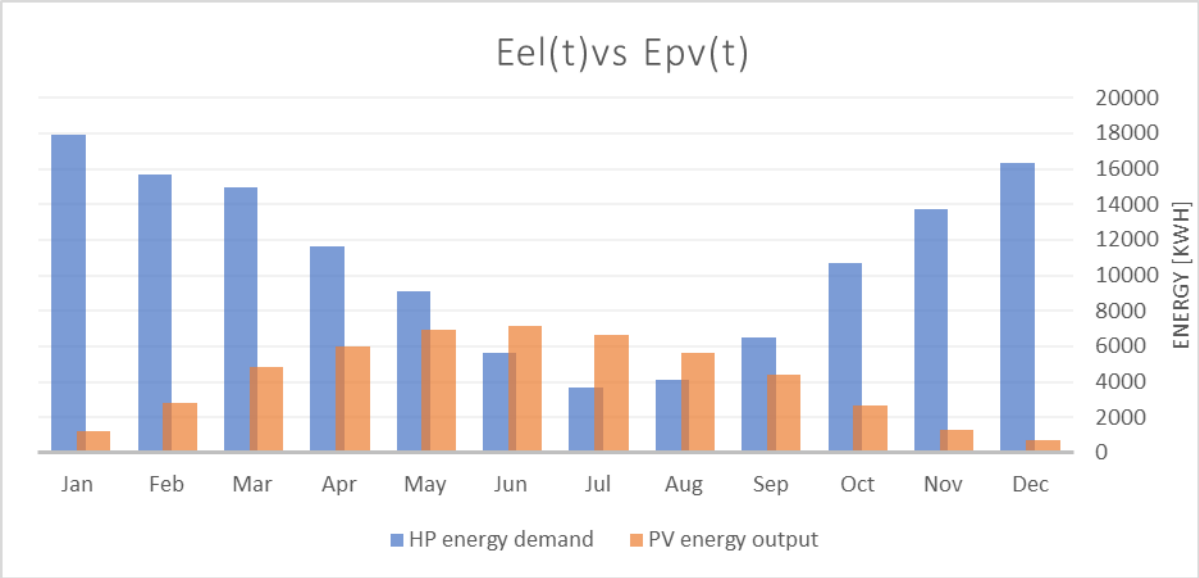

Figure 39 Energy required to run the heat pump compared to the output from the PV array.

The demand is prognosed to be entirely covered by the PV array output during the summer months. However, the appropriate battery system would be needed for that purpose due to irradiation variations during the day. The energy storage system should be able to supply a required daily energy load for a heat pump in summer day which is 200 kWh. Winter months require significand amount of load to run the heat pump from grid. The total annual output from the PV system is estimated to be 50242 kWh, which reduces annual energy that needs to be supplied from grid to 79575 kWh.

3.6.10. Battery sizing

The capacity of storage battery can be expressed as [29]:

$$C_b = \frac{E_{load} * d}{V_b * DOD * \eta_B}$$

Where: E_{load} is the daily average load for summer months, V_b- is the battery bus voltage, d- number of days of autonomy, DoD – depth of discharge

$$E_{load} = 150 * 1.4 = 210 \frac{kW}{day}$$

For the customer grade applications, the highest voltage is from up to 60 V. For this system 48 V is chosen. The battery should secure supply for 1 day in summer, so the days of autonomy is 1. Recommended min depth of discharged is 60 %. The efficiency of lead-acid batteries is 80% when considering ampere-hours.

$$C_b = \frac{210000 * 1}{48 * 0.6 * 0.8} = 9115AH$$

2 parallel strings of (24) 2Volts modules at 4860 AH was chosen ().

System voltage=24*2=48V

System capacity=2*4860=9720

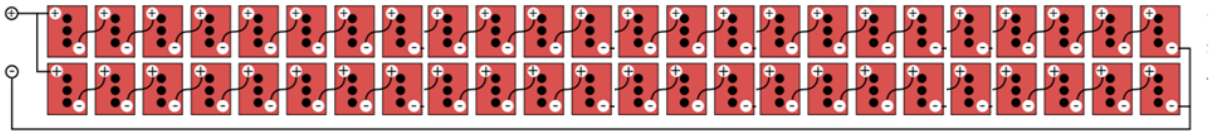

Figure 40 Schematic of batteries set [34]

3.6.11. Charge Controller

Maximum Power Tracking Controller (MPTC) was chosen (Appendix 6). The data input for calculation summarised in the Table 13.

Table 13 Input data for sizing MPPT Controller

PV	
Number of PV modules	n_{pv} =150
Open-circuit voltage	V_{oc} =37.1 V
PV Array peak size	$P_{n,array}$ =(150*235) 35250W
MPPT Charge Controller	
Max PV array open-circuit voltage	$V_{oc,max}$ = 600 V
Rated charge current	I_{ch} = 80 A
Battery	
Nominal voltage	V_b =48 V

Maximum number of modules that can be used in series based on the controller's max Voc

$$\frac{V_{oc,max}}{V_{oc}} = \frac{600}{37.1} = 16.17$$

16 PV modules in series is the maximum.

Total max output from controllers can be calculated as:

$$\frac{P_{n,array}}{V_b} = \frac{35250}{48} = 735A$$

Number of controllers required:

$$\frac{735}{80} = 9.18 = 10$$

10 controllers required connected in parallel as on Image 3. Each controller will be wired to separate array composed from 1 string and max 16 modules in series.

Image 3 Controllers connected in parallel [35]

3.6.12. Inverter selection:

Suggested inverter size is equal to the nominal PV array power output. Output power of around 35 kW is needed. 5 inverters with nominal power of 6.8kW, connected in parallel were chosen. Specification can be found in A.

4. Economic Analysis of the project

4.1.1. Profitability indices

Payback period- Indicates the length of the time required to recover the cost of an investment [36]. It is the number of years that it takes for the energy savings to of

$$PP = \frac{C_0}{C_{income}}$$

C_0 −Initial investment

C_{income} − Cash in-flows. Including the savings in energy generation using alternative technology

Net Present Value – Value of Future cash flows (positive and negative) over the entire life of an investment discounted to the present [37]

$$NPV = -C_0 \sum_{i=1}^{T} \frac{C_i}{(1+r)^T}$$

C_i −Cash flows

r −Discount rate

T −time

Internal Rate of return- discount rate that makes the net present value of a project 0. In other words, it is the expected rate of return that will be earned on a project investment [37].

$$\mathbf{0} = C_0 + \frac{C_1}{(1+IRR)^2} + \frac{C_2}{(1+IRR)^2} + \cdots + \frac{C_n}{(1+IRR)^2}$$

$$\mathbf{0} = NPV = \sum_{i=1}^{n} \frac{C_n}{(1+r)^T}$$

Financial value of investment was evaluated using 3 indicators: NPV, IRR and PP. The project lifetime is assumed to be 20 years. 2 scenarios where considered:

- Scenario1 Ground Source Heat Pump,
- Scenario3 GSHP+ PV array grid connected with Batteries

All calculations performed using Excel spreadsheet according to methodology described above.

Cash flows was calculated according for every year using to the formula:

$$CF = S + Rhi - G - I_{cost}$$

Where: S-Savings for the heat pump heating system, for PV, Rhi- Renewable Heat Incentive incomes, G-cost of heat generation, I_{cost}- total investment cost (only for the first year)

4.1.2. Investment Costs

Investment costs include prices of heat pump, borehole array, PV system with storage, thermal storage. Heat pump and Thermal storage prices excluding VAT are given by producers. Borehole heat exchanger installation costs including the array and all connection was advised on the installer website for every kW installed [38]. Cost of PV system was calculated based on the data available on the Government website from Department for Business, Energy & Industrial Strategy. The data was sourced from the Microgeneration Certificates and the average cost per kW installed includes the cost of the solar PV equipment, cost of installing and connecting to the electricity supply with VAT. Cost of PV batteries, inverter and charge controller was found in the producer price lists, excluding VAT. To all the prices without VAT, 20 % of product value was added to calculate total price. It is assumed that maintenance costs of both HP and PV is covered by producer warranty, so It is not included in the spending.

The labour cost for both borehole heat exchanger and PV system is included in given price per kW. All Investment cost data summarised in the Table 14.

Table 14 Investment Cost

	Units	**Price per unit**	**Number of units**	**Total price with VAT**
Heat Pump Exl.VAT	£/device	94070	1	112884
Borehole Cost Exl.VAT	£/Kw	1400	190	319200
PV cost Inc. VAT	£/Kw	1153	35	40355
Thermal Storage Inc. VAT	£/device	1802	1	2162
PV Batteries Inc. VAT	£/device	1500	24	36000
Inverter Exl. VAT	£/device	3540	5	21240
Charge controller Exl. VAT	£/device	1062	10	12744
VAT	%	20		

Other input parameters

Annual saving is calculated as the amount of money saved with implementation of renewable energy heating system that would have been spent using conventional electric system. Total annual heating from the taken from the simulation is 617880kWh.

The average electricity price per unit by Scottish Power for Glasgow are 18.332p/kWh day and night rate are: 8.50/kWh which gives the average rate of 13.416p/kWh. The efficiency is 100 % therefore, total generation cost estimated if the building were heated by conventional electric system can be calculated as:

$$G_{el,a} = 13.41 * 10^{-2} * E_{h,a} = 82858£$$

The generation cost for Heat pump system can be calculated as:

-For the system with heat pump only, and PV without batteries:

$$G_{hp,a} = 13.41 * 10^{-2} * E_{HP,a}$$

- For the system with PV with added batteries

$$G_{hp,a} = 13.41 * 10^{-2} * (E_{hp,a} - E_{pv,a})$$

The annual saving using the Heat pump system is:

$$S = G_{el,a} - G_{hp,a}$$

Feed -In tariff for the energy from PV according to FIT scheme is 4.17pence/KWh according to Ofgem tariffs [39]. Feed -in tariff according to RHI scheme. The feed-in tariffs for the heat pump system are: 9.36p/kWH for Tier 1(15% of year running at capacity of HP) and 2.79p/kWh (rest output for the year). FIT's or RHI's are free of tax.

So, the Annual incomes can be calculated as:

$$\text{Rhi} = 9.36 * 10^{-2}(1314 * 240) + 2.79 * 10^{-2} * \left(\text{E}_{\text{dem,,a}} - (1314 * 240)\right)$$

To calculate incomes and outcomes for future years the payment needs to be increased every year by inflation rate which is assumed to be 3% compared to the previous rate.

4.1.3. Scenario1: Ground Sourced Heat Pump

Heat pump is the heat source at the building and the total energy to drive it is taken from the grid. There are no additional renewables in the system. The annual cash flows for the first year of operation summarised in the Table 15. Results below in the Figure 41 and Table 16

Table 15 Input parameters for Scenario1

Investment Cost	I	434 246	£
Energy required by HP	$E_{HP,a}$	129816	kWh
Heat pump generation cost	$G_{hp,a}$	17408	£
Savings	S	65450	£
RHI Income	Rhi	37 958	
Inflation	i	3	%
Discount Rate	r	3.5	%

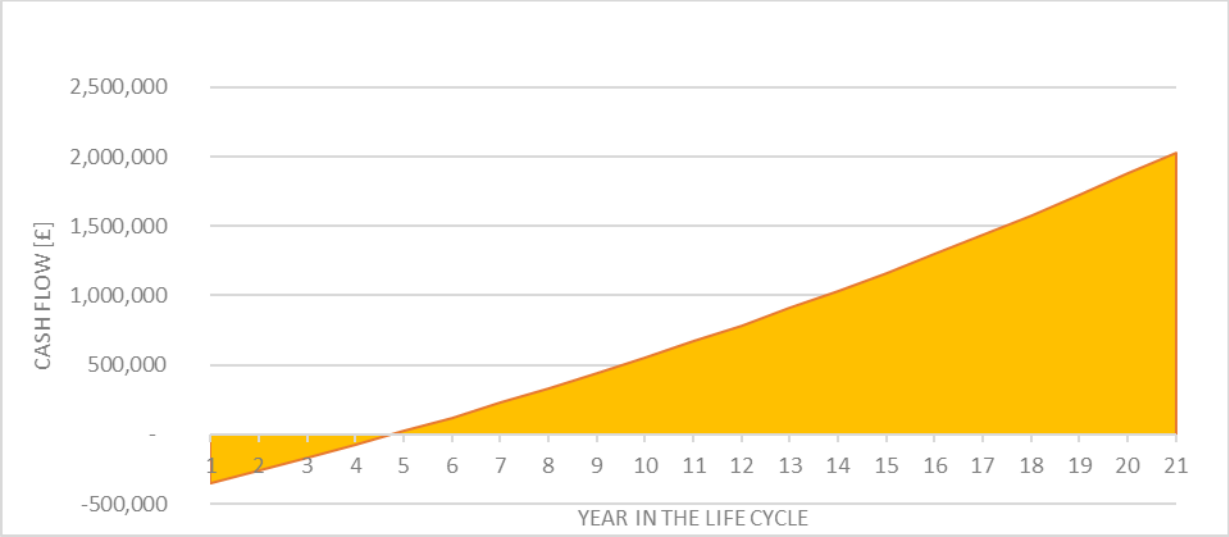

Figure 41 Cumulated cash flows for Scenatrio1

Table 16 Values of financial profitability factors for Scenario 1

PP	5.05	years
NPV	1 287 120	£
IRR	28.11	%

4.1.4. Scenario2: GSHP + Grid connected PV System with Storage

For this scenario there is going to be additional cost increased by inflation rate for new battery bank as the average life of chosen batteries is 15 years. The annual cash flows for the first year of operation summarised in the Table 17. Results below in the Figure 42 and Table 18

Table 17 Input parameters for Scenario2

Investment Cost	I	544 585	£
Additional after 15 years	I_2	52 200	£
Energy required by HP	$E_{HP,a}$	79575	£
Heat pump generation cost	$G_{hp,a}$	10671	£
Savings	S	72187	£

RHI Income	Rhi	37 958	
Inflation	i	3	%
Discount Rate	r	3.5	%

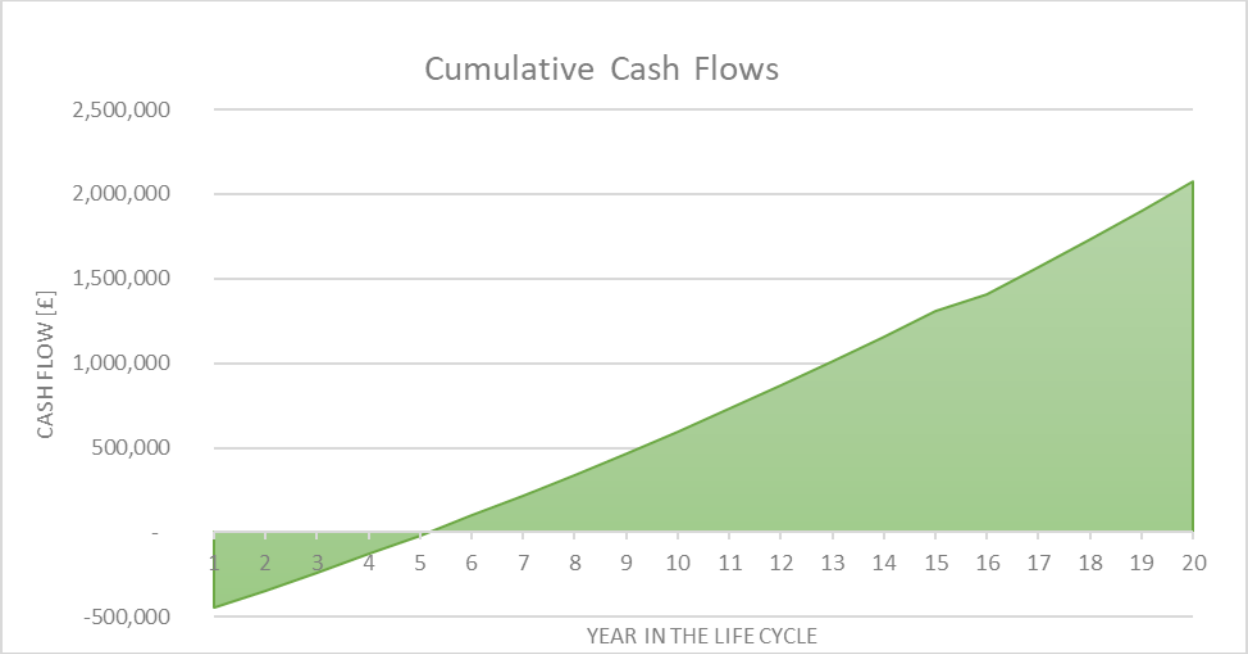

Figure 42 Cumulated cash flows for Scenatrio2

Table 18 Values of financial profitability factors for Scenario 2

PP	5.47	years
NPV	1 415 317	£
IRR	25.49	%

4.1.5. Summary of Financial Analysis

Payback period shows the length of time required to recover the investment cost. In both scenarios the payback period is around 5 years. Scenario 2 have obviously bigger investment costs because of PV system components and the payback period is slightly higher. However, the difference is relatively small which seems to be offset by bigger savings and lower annual energy costs comparing to heat pump system driven only from the Grid. RHI scheme incomes reduces the payback period approximately by half.

NPV shows present value of investment based on expected income from that investment in future years reduced by cost of the project. Its value should be positive to consider project as

successful. For the analysed project income was considered as the cash value of energy savings triggered by use of renewable heat source and payments received from the RHI scheme. Saving are not real incomes, it just a measure how much less would be spent for energy. Analysis shows positive values for both scenarios, which means that both options can be considered as good investments and will generate positive outcomes. Scenario 2 have higher value than Scenario 1, which indicates that the configuration with grid connected PVs and battery storage is more profitable option, despite the higher investment cost.

Internal rate of return is a percentage rate earned on each invested currency unit. It is the interest percentage that investor is going to receive over the time of the project. Again, both Scenarios have good values of IRR and both projects can be accepted. However, Scenario 1 have slightly higher IRR comparing to Scenario2. NPV and IRR provided conflicting results, which might be caused by differences in investment costs for each scenario. As both IRR rates have relatively similar values it is ok to choose the option with higher NPV as the more profitable option, which it that case is Scenario2: Heat pump + grid connected PV system with a battery storage.

5. Environmental Concerns

5.1.1. Ground Source Heat Pump Environmental Impact

Heat pump environmental impact was well described in the report published by European Heat Pump Association [40]. Evaluation of heat pump needs to take into account indirect emissions related to the generation of electricity that is used to operate the heat pump, as well as direct emissions of refrigerant.

Indirect emissions

Highly efficient heat pumps compared to conventional boilers will reduce use of fossil fuels and reduce emission of the greenhouse gasses and other pollutions locally. Heat pumps are not emission free devices as they are associated with indirect emission by using electricity from the grid. The level of emission depends on emission rate at the electricity plant site. In general emission from power plant are lower than from local boilers and furnaces. Indirect emissions from heat pumps will heavily depend from:

- Efficiency of the heat pump (COP)
- Efficiency of the power plant

Direct Emission

Heat pump contribute to direct emission by refrigerant leakage over the lifecycle that occurs during operation and demolition of the device. Impact of those leakages depends of the refrigerant used.

Most established method to calculate contribute of greenhouse gas emission from refrigeration and heat pump is called TEWI which stands for Total Equivalent Warming Impact. The method calculation integrates direct and indirect greenhouse gas emissions over the whole lifetime into a single number expressed as:

$$TEWI = (n * L_r * m_r * GWP) + (n * E_{annual} * EF) + (L_{demolition} * m_r * GWP)$$

n-equipment lifetime[years], L-annual leakage rate [%], m-refrigerant charge [kg], GWP-global warming potential [kgCO2/kg refrigerant], E_{annual} −annual energy use[kWh/year], EF-emission factor driving energy[kgCO2/kWh], $L_{demolition}$ −refrigerant loses during demolition[%].

TEWI calculated for considered scenarios and the base case of conventional electric heating using input parameters summarised in the Table 19 and the results displayed on the Figure 43

Table 19 Input parameters for TEWI calculations

GWP for R410A	1725 kgCO2/kg
m of R410A	60.5 kg
n	20 years
L [41]	3.8%
$L_{demolition}$ [41]	15%
EF [42]	0.3072 kgCO2/kWh
E_{annual} for Scenario1	129816
E_{annual} for Scenario2	79575

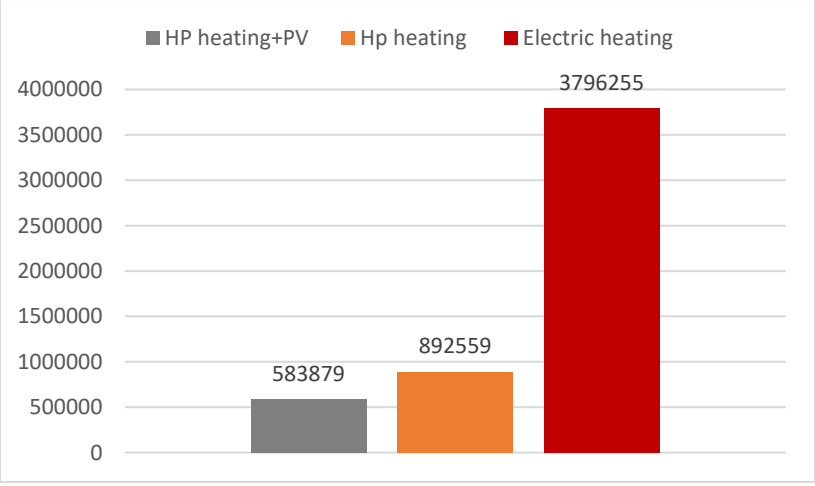

Figure 43 TEWI calculated for considered scenarios and conventional electric heating

The obtained results show that use of heat pump instead of conventional heating will allow to reduce the greenhouse gases emission by 76 %. Additional PV system associated with the heat pump reduces the emission from the heat pump by 35%.

The other part of heat pump that can cause environmental implications is the heat exchanger [43]. The main risks associated with the heat exchanger placed in the ground are:

- Undesirable temperature change in the ground and the water environment which impacts on water quality or aquatic ecology
- Depth systems can result in the interconnection of different aquifers during drilling affecting water quality or flow
- Closed loop systems may contain thermal transfer fluids which are toxic and can pollute groundwater if they leak.

The main risk occurs during the drilling and installation process so before the process starts it is highly recommended to seek the advice of qualified hydrogeologist to understand the geology and hydrology in order to anticipate and mitigate any problems.

5.1.2. PV System Environmental Impact

Solar Panels

After the installation process, solar modules produce emission-free energy for more than 20 years, depends of the lifetime of the system. Although PV's doesn't cause any operating emission there is an impact on environment related to manufacturing process. Comparing to other forms of generation solar panels require more energy up front to produce it. Manufacturing require combining multiple materials with high precision and strict conditions- all of this require lots of up-front energy. Another factor causing negative environmental during manufacturing is use of use of hazardous chemicals involved in crystalline PV cell production, which need to be properly disposed. The other issue is a recycling of panel, which is not a major problem now but will be in the future as the systems have the finite lifetime and they will need to be replaced. As it was mentioned before the modules are produced from combination of materials and the recycling might be challenging [44].

Lead-acid batteries

Environmental impact of batteries is related to the manufacturing process and can also appear during operation due to inappropriate usage or accident events. Generally, lead-acid batteries consist of electrolyte, lead and lead alloy grid, lead paste, organics and plastic which includes

lots of toxic, hazardous, flammable and explosive substances. Those materials are related to the risk of pollution, fire, explosions, contaminating of the environment and damaging ecosystems as well as they can be hazard to humans [45].

When PV System is incorporated with electric driven heating like heat pump system it has indirect positive impact on emissions of greenhouse gases because it can reduce the amount of electricity needed to run the heat pump from grid. Batteries can improve the reduction even more as they can balance the load by storing the energy and releasing it when its needed. Resulted reduction of emission for designed system was shown previously on the Figure 43.

6. Discussion

This chapter reviews the main outcomes and findings of the project against the aims. It also gives the overview of the assumptions and limitations of the project and suggests the future work that could be built on the thesis to address project constraints.

The main aim of the project was to design and analyse a low-carbon and affordable heating generation system for a high-rise residential building. Ground heat pump with borehole heat exchanger was designed together with roof-mounted PV array, connected to utility grid and supported by a battery bank. Economical evaluation proved that replacing conventional electric heating with central heat pump would bring significant savings in the energy and the cost reduction. The investment costs of the project were quite high in both cases, with and without PV system, however the Renewable Heat Incentive Scheme payments and lower annual energy costs allowed to achieve promising payback period just over 5 years. NPV analysis shows that additional PV system with battery storage would bring bigger savings in energy use, hence more profits for the investment during the 20 years of project lifetime. Environmental evaluation shown that there is huge reduction of CO2 emission related to change from conventional electric heating to heat pump. Estimating scenario with added PV system proved that the emissions decreased even more when comparing to the system only with a heat pump.

The project focused on the generation side of the system and internal heating in dwelling was out of the scope. Design of the internal space heating system is a good proposal for a separate project.

In the chapter ‘Heating and DHW loads’ for the Esp-r energy simulation the weather file from Dundee was used which is in the distance about 100 km from the side. The weather file could be replaced in the Esp-r model by the one from Glasgow, to obtain more accurate heating demand profile. However due to unavailability of a free version of the file, it wasn’t changed.

After reviewing temperatures, it was found that the climate of Dundee is similar enough to be used. The second assumption taken in terms of modelling of heat load was that the model was created only for one floor of the building due to restricted number of thermal zones in the esp-r tool. Hence the simulation was performed for one floor of the building and the heat load was then scaled up for the whole building according to the number of floors. Due to repetitive construction and unchangeable layout of flats on each floor the estimation is considered to be good enough for the purposes of the project.

In the chapter including calculations of required length of the heat exchanger, the ground properties and the borehole resistance were assumed as the typical occurred values. For medium to large-sized systems, these properties are often estimated using an *in situ* thermal response test (TRT). Uncertainties in the estimated parameters can result in under- or over-sized borehole systems. Thermal response test is usually done by qualified hydrogeology consultants and is highly recommended for this project.

Part of the project with PV includes the calculations of a monthly energy output based on calculated power output for representative day of the month. It was assumed that every day in given month have the same daily energy output. That is an estimation as ideally the energy output for each day would need to be calculated individually. However due to restricted irradiance data and time constraints those detailed calculations were omitted.

In the financial part of the project the grid connected system without batteries could be additionally considered as a separate scenario. However, that was limited by the solar energy estimated as the same for each day of the month, which would give basically the same surplus energy for every day of the month. That could lead to over or under estimation of exported energy. To properly calculate surplus energy hourly energy output for every day of the month would need to be known. In the analysis savings are treated as positive cash flows however it is not the real income. It is just a measure of how much less would need to be spent for energy with alternative generation system.

Environmental evaluation of the project focuses mainly on reduction of emissions due to operation of different systems mentioned in 2 considered scenarios and the base case which is conventional electric heating. Environmental impact assessment should include impact of each element of the system through their entire life cycle from raw material extraction through transport, manufacturing and use all the way to their end of life. Complete environmental impact assessment of the system is another idea for additional research that has risen from this project.

Generation of energy from renewable sources is always related to uncertainties due to nature of renewables that are dependent from changing climate conditions.

In this case, the ground heat pump with borehole heat exchanger, the temperatures of ground are stable, so the power yield from heat exchanger have a steady value as well. However, the actual heat output from 1 meter of the borehole rarely corresponds to the one assumed at the design stage of the installation, where the ground parameters are assumed. Therefore, after drilling the first borehole and testing real thermal efficiency, the borehole design is usually corrected by reducing or increasing the total length of the vertical collector. In calculations of electric load, it was assumed steady COP value, declared by heat pump producer, for the inlet brine temperature of 5°C. In case of heat pump with geothermal probes it gives the realistic results as the desired temperature of brine can be achieved by correct design of the exchanger length and it has fairly stable value through all year.

DC yield of PV module depends on the module characteristic and operation conditions. The most influencing effects are irradiance, angle of incidence and operating temperature. In the project the irradiance data for exact location was used to calculate irradiance on the inclined surface, then the module temperature was calculated relating to ambient temperatures. Power output for every hour of the day in reference month was calculated according to obtained irradiance and surface temperature. Obtained output energy factor for every month was then used to calculate total energy output for reference year. The approximation of the PV output was detailed enough to obtain credible energy output for reference year. However, for long term approximation is uncertain as the climate changes and so as the irradiance which is dominating factor in estimating energy output from PV modules. There are some models in reference literature that allows to calculate long- term yield uncertainties based on statistics and historical data, and perhaps that would decrease the error. However, there always going to be some level of error in any prediction.

7. Conclusions

The section lists key findings of the project related to design and analysis.

Thermal store can be used to reduce the nominal required capacity of heat pump required in the system therefore the length of the heat exchanger needed to extract sufficient amount of heat. COP of the heat pump is not a fixed value. It depends primarily on the temperatures of the evaporator and the condenser. Hence the temperatures of brine that is supplied to the heat

pump from ground and the temperature of heating circuit deliver to heat pump to take over the heat from condenser determine the effectiveness of the heat pump. The closer the two temperatures are to each other the higher COP. Therefore, correctly sized length of heat exchanger is crucial for the ground heat pump system. Undersized length of boreholes will result in lower temperature of the heat transfer fluid which will then lower the COP of heat pump and that will result in the heat load deficit. That indicates how important the size of the heat exchanger is for the worst ground conditions.

Real power output from panels depends from the location of the system and climate conditions. Power output from PV modules depends primarily from the intensity of irradiance on inclined surface and it varies hourly. Secondly the temperature of the surface influences the efficiency of the module which drops with temperature rise. The energy output from the PVs is inversely proportional to the energy that is required to run the heat pump. In other words, the energy from the PV array increase in the summer and decrease in winter while the heat pump energy load increases in winter and decreases in summer. In Winter, the heat pump would operate using the energy taken from the grid while in summer the energy from PV's could be sufficient to supply the heat pump. Because of the daily variations of the power output from PV array, battery system with at least 1 day of autonomy is needed in the system to fully take advantage of energy produced on the site.

The investment cost of the system is dominated by the cost of heat pump and borehole heat exchanger and it is quite high comparing to competitive heating systems. However, the financial analysis shown relatively short payback period that indicates the savings achieved from the use of the heat pump comparing to conventional electric system are significant. It turned out that RHI scheme incomes helps to reduce payback period of investment by half, from about 10 to 5 years. Adding the PV system and battery storage to the heat pump heating system would not cause significant higher payback period and would bring more savings in energy costs.

Analysis of emissions shows that use of the heat pump system instead of conventional electric heating would bring about 76% of reduction in greenhouse gasses emission and added PV system would decrease the emission from heat pump by additional 30 %. From both points of view financial and environmental the system with heat pump and grid connected PV system with backup storage is more effective option.

8. Future work

There are four main areas for the future research that could be built on the project.

Firs of all is the dynamic simulation of the system. Modelling is a way to validate the initial design and optimize the system. It allows to test performance of designed system due to different environmental conditions. The most popular software mentioned in reference literature for simulation of combined solar and ground source heat pump system is TRNSYS. The software uses modular approach and it's a flexible tool for hybrid systems. Other software that could be used is EnergyPro or Matlab/Simulink.

Secondly, the redesign of heating system in dwelling. Low temperature heating requires different system design mainly to ensure that the radiators can deliver the same amount of heat at lower temperature as a traditional water heating system. Popular technology used for that kind of systems is floor heating. Additionally, the distribution of the heat from central heat pump to dwellings needs to be considered (Heat Interface Units).

Thirdly, an investigation of most effective operation of the heat pump trough the control of the heat pump and smart demand side management. The national Grid is able to broadcast when the supply electricity is much higher than demand, so the Grid can sell electricity much cheaper than usual. Adequately the price of electricity will increase when demand is higher than supply. For the heating with heat pump there is an opportunity to reduce costs of heating by responding to the price signals from Grid. The heat pump would need to be connected to the grid trough via the IoT technology, which stands for Internet of Things and allows the instant communication of information between devices connected to the internet. Demand Site Management implemented trough IoT and together with control of the heat pump is another topic for future research.

The last proposal for future research is a study of an integration of hybrid PV/thermal modules on the source side of the heat pump. Installing thermal modules on the back of PV cells can increase the electricity production as the modules are cooled. It is also possible to implement borehole thermal energy storage that could increase the heat capacity of boreholes by injection of solar thermal energy. Solar thermal injection could reduce required borehole length.

Appendix 1 Floor Plan of Tower Building

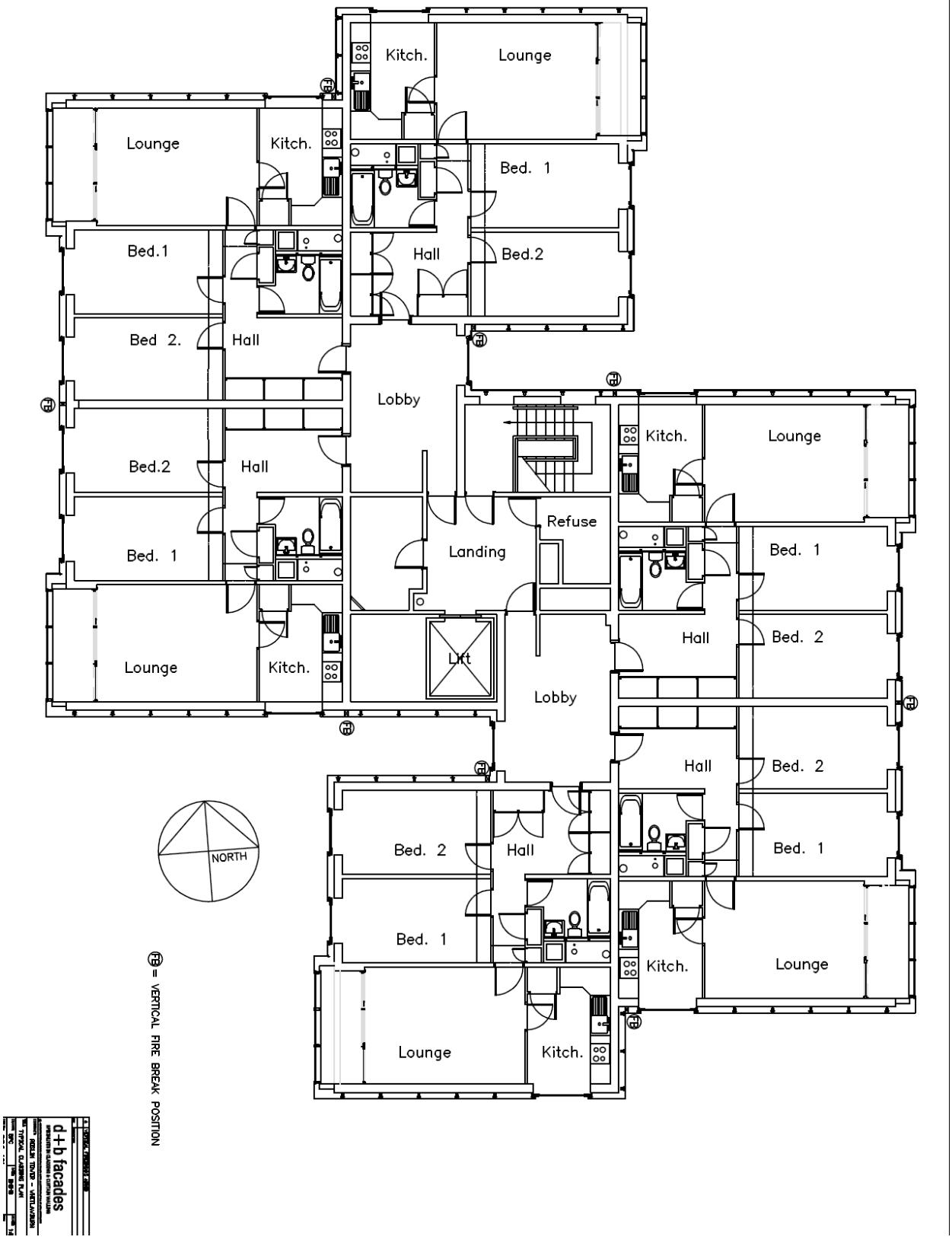

Appendix 2Heat Pump Specification

Vitocal 300-G Pro brine/water heat pump

Vitocal 300-G Pro	Type	BW 301.B090	BW 301.B120	BW 302.B090	BW 302.B120
Output data (to EN 14511, B0/W35 °C, 5 K spread)					
Rated heating output	kW	93	121	89.4	117.7
Cooling capacity	kW	74.5	96.4	72	93.8
Power consumption	kW	19.5	24.8	18.3	24.4
Coefficient of performance ε (COP) in heating mode		4.77	4.83	4.88	4.8
Dimensions					
Length	mm	1343	1343	1343	1343
Width	mm	911	911	911	911
Height	mm	1650	1650	1650	1650
Weight	kg	700	800	705	810
Number of compressors	pce	1	1	2	2

Vitocal 300-G Pro	Type	BW 302.B150	BW 302.B180	BW 302.B250
Output data (to EN 14511, B0/W35 °C, 5 K spread)				
Rated heating output	kW	145	180	240
Cooling capacity	kW	117	145.4	191.4
Power consumption	kW	31.5	39.2	50.4
Coefficient of performance ε (COP) in heating mode		4.6	4.6	4.76
Dimensions				
Length	mm	1932	1932	1932
Width	mm	911	911	911
Height	mm	1650	1650	1650
Weight	kg	1130	1190	1300
Number of compressors	pce	2	2	2

SCHOTT Solar POLY™ Polycrystalline Solar Modules

SCHOTT POLY™ 220/225/230/235/240

At a glance

- Industry leading warranty
- Narrow output tolerance
- Long-term reliability
- High resistance to mechanical loads
- Up-to-date features
- Environmentally friendly

SCHOTT Solar manufactures modules in Albuquerque, New Mexico, and other global production facilities.

The modules from Albuquerque:

- Qualify as a domestic end product under the Buy American Act (BAA)
- Qualify as a U.S.-made end product under the Trade Agreement Act (TAA)
- Qualify as a domestic manufactured product under the American Recovery & Reinvestment Act (ARRA)

SCHOTT Solar has been a leading global developer and manufacturer of solar products for over 52 years. Engineered in Germany, the high quality SCHOTT Solar PV modules are extremely durable and reliable as demonstrated in several important ways:

Industry leading warranty: SCHOTT Solar offers an industry leading linear power output warranty for 25 years in addition to five years warranty for any defects in materials or workmanship. This enhancement provides 6% more guaranteed power over the 25 year period compared to standard step-down warranties common in the industry.

Narrow output tolerance: SCHOTT Solar POLY™ modules are among the industry leaders in lower output tolerances. SCHOTT Solar sorts all modules to a positive tolerance (minus zero watts) which provides for a stable, high energy output you can feel secure in.

Long-term reliability: SCHOTT modules are environmentally tested to double the industry certification standards for thermal cycling and damp heat tests to ensure consistent and superior performance over the long term. In addition, SCHOTT has performance data from over 25 years of actual field testing that supports our high quality products.

High resistance to mechanical loads: SCHOTT Solar modules are tested to an extreme loading pressure of 5,400 Pa to ensure additional security for your investment.

Up-to-date features: SCHOTT Solar modules offer up-to-date electrical features such as double insulated PV cables for use with transformerless inverters and locking connectors.

Environmentally friendly: Due to our concern with job site waste and disposal costs, we bulk pack our modules in a manner that significantly reduces cardboard waste.

SCHOTT solar

Technical Data

Electrical Data

Module type		SCHOTT POLY™ 220	SCHOTT POLY™ 225	SCHOTT POLY™ 230	SCHOTT POLY™ 235	SCHOTT POLY™ 240
Nominal power [Wp]	P_{mpp}	≥ 220	≥ 225	≥ 230	≥ 235	≥ 240
Voltage at nominal power [V]	V_{mpp}	29.7	29.8	30.0	30.2	30.4
Current at nominal power [A]	I_{mpp}	7.41	7.55	7.66	7.78	7.90
Open-circuit voltage [V]	V_{oc}	36.5	36.7	36.9	37.1	37.3
Short-circuit current [A]	I_{sc}	8.15	8.24	8.33	8.42	8.52

STC (1,000 W/m², AM 1.5 cell temperature 25°C)
Power tolerance (as measured by flasher): -0 Watts / +4.99 Watts

Data at Normal Operating Cell Temperature (NOCT)

Nominal power [Wp]	P_{mpp}	158	161	165	169	172
Voltage at nominal power [V]	V_{mpp}	26.7	26.9	27.1	27.2	27.4
Current at nominal power [A]	I_{mpp}	33.3	33.5	33.7	33.9	34.1
Open-circuit voltage [V]	V_{oc}	6.53	6.60	6.67	6.75	6.83
Temperature [°C]	T_{NOCT}	45.5	45.5	45.5	45.5	45.5

NOCT (800 W/m², AM 1.5, windspeed 1 m/s, ambient temperature 20°C

Data at Low Irradiation

At a low irradiation intensity of 200 W/m² (AM 1.5 and cell temperature 25°C) 97% of the STC module efficiency (1000 W/m²) will be achieved.

Temperature Coefficients

Power [%/°C]	-0.44
Open-circuit voltage [%/°C]	-0.32
Short circuit current [%/°C]	+0.04

Characteristic Data

Solar cells per module	60
Cell type	6" (156 mm x 156 mm), full square
Front panel	Low-iron solar glass
Frame material	Anodized aluminum
Connection	Junction box with 3 bypass diodes PV WIRE, 43.3" (1,100 mm) x 4 mm² TYCO SolarLok connectors

Dimensions and Weight

Dimensions	66.34" (1,685 mm) x 39.09" (993 mm) tolerance ± 0.118" (3 mm)
Thickness	1.97" (50 mm) tolerance ± 0.04" (1 mm)
Weight	Approx. 41.5 lbs (18.8 kg)

Limits

System voltage [V_{DC}]	600
Maximum reverse current [A]*	15
Operating module temperature	[°C]
Maximum load (lbs/ft²)	75
Fire classification	C

** No external current greater than V_{oc} shall be applied to the module.*

Qualifications

The SCHOTT POLY™ 220/225/230/235/240 Watt modules are certified to and meet the requirements of UL 1703.

SCHOTT Solar reserves the rights to make specification changes without notice. For detailed product drawings and specifications, please contact SCHOTT Solar or an authorized reseller.

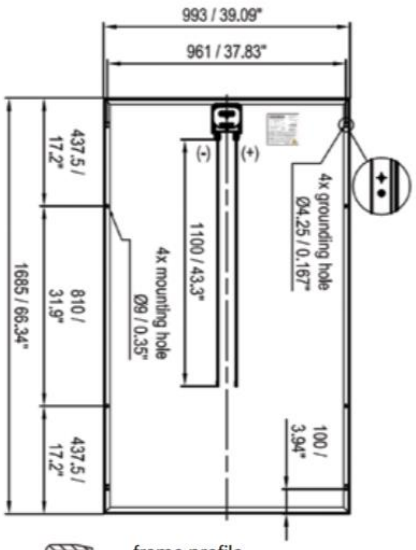

frame profile

All dimensions in mm/inches

SCHOTT Solar PV, Inc.
U.S. Production Facility
5201 Hawking Drive, SE
Albuquerque, NM 87106
Toll free: 888-457-6527
Email: sales@us.schottsolar.com

SCHOTT solar

Rolls

FLOODED DEEP CYCLE BATTERY — 2 YS 62P

Series	5000	Warranty	10 Years
Volts	2	BCI	SPEC
Cells	2	Plates/Cell	31
Terminal Type		Flag RR	
Included Hardware		S/S Hex Cap Screw, Nut, Lock & Flat Washer	
Size & Thread		5/16"-18 x 1-1/2"	
Cables		19" 4/0 interconnect cables *RE incl.	

Charge

Charge Voltage Range	2.45-2.5 V/cell @ 25°C (77°F)
Float Voltage Range	2.25 V/cell @ 25°C (77°F)
Self-Discharge Rate	5%-10% per month at 25°C (77°F)

Capacity

Cold Crank Amps (CCA) 0°F / -17°C	5741
Marine Crank Amps (MCA) 32°F / 0°C	7176
Reserve Capacity (RC @ 25A)	11664 Minutes
Reserve Capacity (RC @ 75A)	3888 Minutes

Hour Rate	Capacity / AMP Hour	Current / AMPs
@ 100 Hour Rate	**6853 AH**	**68.53 A**
@ 75 Hour Rate	**5042 AH**	**70.02 A**
@ 50 Hour Rate	**4663 AH**	**93.25 A**
@ 20 Hour Rate	**4860 AH**	**243 A**
@ 15 Hour Rate	**4520 AH**	**301.32 A**
@ 10 Hour Rate	**4034 AH**	**403.38 A**
@ 8 Hour Rate	**3791 AH**	**473.85 A**
@ 5 Hour Rate	**3256 AH**	**651.24 A**
@ 1 Hour Rate	**1652 AH**	**1652.4 A**

Amphere hour capacity ratings based on specific gravity of 1.280.
Reduce capacities 5% for specific gravity of 1.265 and 10% for 1.250.

Specifications

Certified System™ — SAI GLOBAL ISO 9001 Quality

Weight	258.5 kg	570 lbs
Length	69.5 cm	27.38"
Width	22.9 cm	9"
Height Inc. Term.	80.3 cm	3163"

Product measurements & weights are calculated based on sample data. Individual specifications are subject to vary due to the manufacturing process, battery components & electrolyte levels.

Electrolyte Reserve	95 mm	3.75"
Container (Inner)	Polypropylene	
Cover (Inner)	Polypropylene - heat sealed to inner container	
Container (Outer)	High Density Polyethylene	
Cover (Outer)	High Density Polyethylene snap fit to outer container	
Handles	Molded	

Cycle Life vs. Depth of Discharge

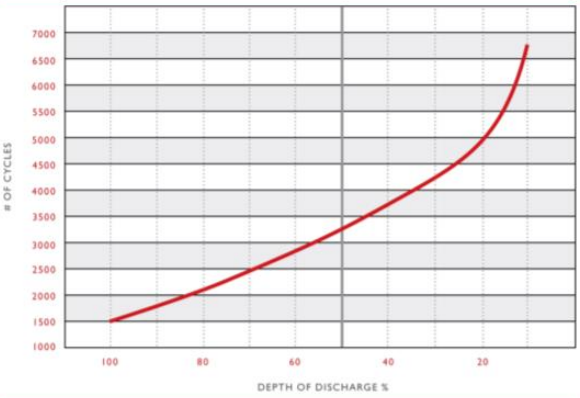

Voltage vs. Depth of Discharge

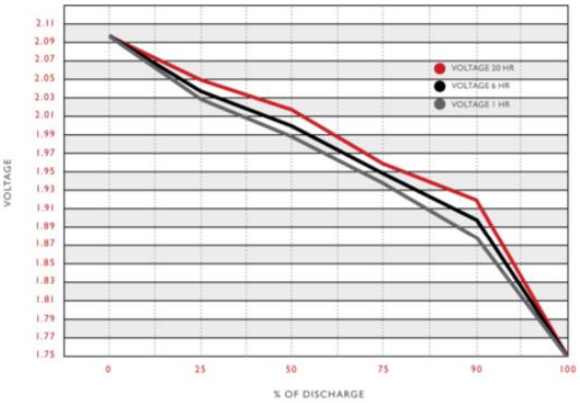

Conext XW+ series (120/240 V)

Device short name	XW+ 5548 NA	XW+ 6848 NA
Inverter AC output (standalone)		
Output power (continuous) at 25°C	5500 W	6800 W
Overload 30 min/60 sec at 25°C	7000 W/9500 W	8500 W/12000 W
Output power (continuous) at 40°C	4500 W	6000 W
Maximum output current 60 seconds (rms)	82 A (120 V); 41 A (240 V)	102 A (120 V); 52 A (240 V)
Output frequency (selectable)	50/60 Hz	50/60 Hz
Output voltage	L-N: 120 V +/- 3%; L-L: 240 V +/- 3%	L-N: 120 V +/- 3%; L-L: 240 V +/- 3%
Total harmonic distortion at rated power	< 5 %	< 5 %
Idle consumption search mode	< 8 W	< 8 W
Input DC voltage range	42 to 60 V (48 V nominal)	42 to 60 V (48 V nominal)
Maximum input DC current	150 A	180 A
Charger DC output		
Maximum output charge current	110 A	140 A
Output charge voltage range	40 – 64 V (48 V nominal)	40 – 64 V (48 V nominal)
Charge control	Three stage, two stage, boost, custom	Three stage, two stage, boost, custom
Charge temperature compensation	Battery temperature sensor included	Battery temperature sensor included
Power factor corrected charging	0.98	0.98
Compatible battery types	Flooded (default), Gel, AGM, Lithium ion, custom*	Flooded (default), Gel, AGM, Lithium ion, custom*
Battery bank range (scaled to PV array size)	440 – 10000 Ah	440 – 10000 Ah
AC input		
AC 1 (grid) input current (selectable limit)	3 – 60 A (60 A default)	3 – 60 A (60 A default)
AC 2 (generator) input current (selectable limit)	3 – 60 A (60 A default)	3 – 60 A (60 A default)
Automatic transfer relay rating/typical transfer time	60 A/8 ms	60 A/8 ms
AC input voltage limits (bypass/charge mode)	L-N: 78 - 140 V (120 V nominal); L-L: 160 - 270 V (240 V nominal)	L-N: 78 - 140 V (120 V nominal); L-L: 160 - 270 V (240 V nominal)
AC input frequency range (bypass/charge mode)	55 – 65 Hz (default) 52 – 68 Hz (allowable)	55 – 65 Hz (default) 52 – 68 Hz (allowable)
AC grid-tie output		
Grid sell current range on AC1(selectable limit)	0 to 40 A (120 V) / 0 to 20 A (240 V)	0 to 48 A (120 V) / 0 to 27 A (240 V)
Grid sell voltage range on AC1 (auto adjusts entering sell mode)	L-N: 105.5 to 132 +/- 1.5 V; L-L: 211 to 264 +/- 3.0 V	L-N: 105.5 to 132 +/- 1.5 V; L-L: 211 to 264 +/- 3.0 V
Grid sell frequency range on AC1 (auto adjust entering sell mode)	59.4 to 60.4 +/- 0.05 Hz	59.4 to 60.4 +/- 0.05 Hz
Efficiency		
Peak	95.7%	95.7%
CEC weighted efficiency	93.0%	92.5%
General specifications		
Part number	865-5548-01	865-6848-01
Product/shipping weight	53.5 kg (118.0 lb)/75.0 kg (165.0 lb)	55.2 kg (121.7 lb)/76.7 kg (169.0 lb)
Product dimensions (H x W x D)	58 x 41 x 23 cm (23 x 16 x 9 in)	58 x 41 x 23 cm (23 x 16 x 9 in)
Shipping dimensions (H x W x D)	71.1 x 57.2 x 39.4 cm (28.0 x 22.5 x 15.5 in)	71.1 x 57.2 x 39.4 cm (28.0 x 22.5 x 15.5 in)
IP degree of protection	NEMA Type 1 Indoor	
Operating air temperature range	-25°C to 70°C (-13°F to 158°F) (power derated above 25°C (77°F))	
Warranty (depending on the country of installation)	2 or 5 years	2 or 5 years
Features		
System monitoring and network communications	Available	
Intelligent features	Grid sell, peak load shave, generator support, prioritized consumption of battery or external DC energy	
Auxiliary port	0 to 12 V, maximum 250 mA DC output, selectable triggers	
Off-grid AC coupling	Frequency control	
Regulatory approval		
Safety	UL1741, CSA 107.1	
EMC directive	FCC and Industry Canada Class B	
Interconnect	IEEE 1547 and CSA 107.1	
Compatible products		
Conext XW + Power Distribution Panel	865-1014-01	
Conext System Control Panel	865-1050	
Conext Automatic Generator Start	865-1060	
Conext MPPT 60 150	865-1030-1	
Conext MPPT 80 600	865-1032	
Conext ComBox	865-1058	
Conext Battery Monitor	865-1080-01	
Conext Battery Fuse Combiner Box	865-1031-01	
Conext Configuration Tool	865-1155-01	

Specifications are subject to change without notice.

Schneider Electric
35 rue Joseph Monier
92500 Rueil-Malmaison, France
Tel: +33 (0)1 41 29 70 00

Life Is On Schneider Electric

Appendix 6 Charge Controller Specification

Device short name	MPPT 80 600
Electrical specifications	
Nominal battery voltage	24 and 48 V (Default is 48 V)
PV array operating voltage	195 to 550 V
Max. PV array open circuit voltage	600 V including temperature correction factor
Battery voltage operating range	16 to 67 VDC
Array short-circuit current	35 A (28 A @ STC)
Max. charge current	80 A
Max. and min. PV wire size in conduit	#6 AWG to #14 AWG (13.5 to 2.5 mm^2)
Max. output power	2560 W (nominal 24 V), 4800 W (nominal 48 V)
Charger regulation method	Three-stage (bulk, absorption, float) plus manual equalization Two-stage (bulk, absorption) plus manual equalization
Supported battery types	Flooded, GEL, AGM, Lithium-ion, Custom
Efficiency	
Max. power conversion efficiency	94% (nominal 24 V), 96% (nominal 48 V)
General specifications	
Power consumption, night time	< 1 W
Battery temperature sensor	Included
Auxiliary output	Dry contact switching up to 60 VDC, 30 VAC, 8A
Enclosure material	Enclosure material: Indoor, ventilated, aluminium sheet metal chassis Knockout Dimensions: 44.0 mm, 35.0 mm , 28.2 mm, and 22.2 mm knockouts for 1-1/4, 1, ¾, and ½ inch trade size fittings
IP degree of protection	IP20
Product weight	13.5 kg (29.8 lb)
Shipping weight	19.5 kg (43 lb)
Product dimensions (H x W x D)	76.0 × 22.0 × 22.0 cm (30.0 × 8.6 × 8.6 in)
Shipping dimensions (H x W x D)	113.39 × 28.68 × 31.90 cm (44.64 × 11.29 × 12.56 in)
Device mounting	Vertical wall mount
Ambient air temperature for operation	-20 °C to 65 °C (-4 °F to 149 °F), power derating above 45 °C
Storage temperature range	-40 °C to 85 °C (-40 °F to 185 °F)
Operating altitude	Sea level to 2000 m (6562 ft)
System network and remote monitoring	Available
Warranty	Five-year standard
Part number	865-1032
Regulatory approvals	
Safety	CSA certified (UL1741, CSA 107.1) and CE marked for the Low-voltage Directive (EN50178)
EMC	FCC and Industry Canada (Class B), CE marked for the EMC Directive (EN61000-6-1, -6-3), C-Tick compliant
Compatible products	
Conext XW+ inverter/charger (230 V)	XW 7048 E product no. 865-7048-61/XW 8548 E product no. 865-8548-61
Conext XW+ inverter/charger (120/240 V)	XW 5548 NA product no. 865-5548-01/XW 6848 NA product no. 865-6848-01
Conext SW (230 V)	SW 2524 product no. 865-2524-61/SW 4024 product no. 865-4024-61/SW 4048 product no. 865-4048-61
Conext SW (120 V)	SW 2524 product no. 865-2524/SW 4024 product no. 865-4024/SW 4048 product no. 865-4048
Conext System Control Panel	Product no. 865-1050-01
Conext Automatic Generator Start	Product no. 865-1060-01
Conext ComBox	Product no. 865-1058
Conext portable installation and configuration tool	Product no. 865-1155-01

Specifications are subject to change without notice.

Schneider Electric
Head Office
35 rue Joseph Monier
92500 Rueil-Malmaison, France
Tel : +33 (0)1 41 29 70 00
solar.schneider-electric.com

Life Is On Schneider Electric

Bibliography

[1] "The Scottish Goverment," 13 01 2012. [Online]. Available: https://www.gov.scot/Topics/Statistics/Browse/Housing-Regeneration/TrendFuelPoverty. [Accessed 02 08 2018].

[2] "Scottish House Condition Survey: 2016. Key Findings," The Scottish Goverment, Edinburgh, 2017.

[3] Hui-Xie, "Legal Regulation of Low-Carbon Economy," *IERI Procedia,* vol. 8, pp. 170-175, 2014.

[4] United Nations, "Sustainable Development Knowladge Platform," 2015. [Online]. Available: https://sustainabledevelopment.un.org/post2015/summit. [Accessed 20 06 2018].

[5] IRENA, "Heat Pumps. Technology Brief," IRENA, 2013.

[6] IRENA, "Renewable Energy Prospects for European Union," European Union & IRENA, 2018.

[7] Viessman, "Technical Manual. Heat Pumps," The Viessman group , 2012.

[8] "Coefficient of Performance / Industrial Heat Pumps," [Online]. Available: http://industrialheatpumps.nl/en/how_it_works/cop_heat_pump/. [Accessed 10 07 2018].

[9] John Allison, Keith Bell, Joe Clarke, Andrew Cowie, Ahmed Elsayed, Graeme Flett, Gbemi Oluleye, Adam Hawkes, Graeme Hawker, Nick Kelly, Maria Manuela Marinho de Castro, Tim Sharpe, Andy Shea, Paul Strachan, Paul Tuohy, "Assessing domestic heat storage requirements for energy flexibility over varying timescales," *Applied Thermal Engineering,* 2018.

[10] A. Arteconi. N.J Hewwit, F. Polonara, "State of the art of thermal storage for demand-side management," *Applied Energy,* vol. 93, pp. 371-389, 2012.

[11] D. L. V. H. R. Philip Eames, "The Future Role of Thermal Energy Storage in the UK Energy Systems: An assesment of the Technical Feasibility and Factors Influencing Adoption," UK Energy Research Centre , 2014.

[12] S.P Kavanaugh, K.D Rafferty, Geothermal Heating and Cooling: Design of Ground-Source Heat Pump Systems, ASHRAE, 2014.

[13] Rehau, "Raugeo System Technology. Innovative Heating, Cooling and Storage Using Ground-Source Energy," Rehau Unlimited Polymer Solutions, 11 2012. [Online]. Available: https://www.rehau.com/download/790486/raugeo-technical-manual-september-2012.pdf. [Accessed 20 06 2018].

[14] Patricia Monzó, Michel Bernier, José Acuña, Palne Mogensen, "A Monthly Based Bore Field Sizing Methodology with Applications to Optimum Borehole Spacing," *ASHRAE Transatcions,* vol. 122(1), 2016.

[15] Florida Solar Energy Center, [Online]. Available: http://www.fsec.ucf.edu/en/consumer/solar_electricity/basics/how_pv_cells_work.htm. [Accessed 15 07 2018].

[16] “Types of PV systems - Hermes Solar LTD,” Hermes Solar LTD, [Online]. Available: http://www.hermessolar.com/en/services/types-of-pv-systems/. [Accessed 13 07 2018].

[17] “Alternative Energy. Alternative Energy Sollutions for the 21st Century,” [Online]. Available: http://www.altenergy.org/renewables/solar/common-types-of-solar-cells.html. [Accessed 10 06 2018].

[18] S. B. Christiana Honsberg, “PVEducation,” [Online]. Available: https://www.pveducation.org/. [Accessed July 2018].

[19] “Wind and Sun specialise in solar PV, wind monitoring, off grid systems and many more wind and solar energy solutions,” Wind & Sun Powering the Future, [Online]. Available: http://www.windandsun.co.uk/information/batteries.aspx#.W3aNW-hKguU. [Accessed 21 07 2018].

[20] Haisheng Chen, Thang Ngoc Cong, Wei Yang, Chunqing Tan, Yongliang Li, Yulong Ding, “Progress in electrical energy storage system: A critical review,” *Progress in Natural Science ,* vol. 19, pp. 291-312, 2009.

[21] F. Peacock, “Lithium Ion Batteries and solar energy storage,” SolarQuotes , [Online]. Available: https://www.solarquotes.com.au/lithiumbatteries.html. [Accessed 15 07 2018].

[22] F. Peacock, “Flow Batteries and Solar Battery Storage,” Solarquotes, [Online]. Available: https://www.solarquotes.com.au/flowbatteries.html. [Accessed 15 07 2018].

[23] “ESP-r, Multi-platform Building Energy Software Tool,” [Online]. Available: http://www.esru.strath.ac.uk/Programs/ESP-r_overview.htm. [Accessed 10 June 2018].

[24] K. V. Ulrike Jordan, “Manual DHWcalc Tool for the Generation of Domestic Hot Water (DWH) Profiles on a Statistical Basis,” Universitat Kassel, Kassel, 2017.

[25] British Standard Institution, “BS EN 12831-3:2017,” BSI, London, 2017.

[26] “Thermal stores, thermal storages, buffer tanks, accumulator tanks, cylinders,” Linszter Ltd, [Online]. Available: https://thermal-store.co.uk/5000l.php#5000l-lvt. [Accessed 10 06 2018].

[27] “Calculation of g-functions with uniform borehole heat extraction rates,” [Online]. Available: https://pygfunction.readthedocs.io/en/v1.1.0/example_uniform_heat_extraction_rate.html. [Accessed 13 July 2018].

[28] M. C. M Bernier, “A semi-analitycal method to generate g-functions for geothermal bore fields,” *International Journal of Heat and Mass Transfer ,* vol. 70, pp. 641-650, 2014.

[29] E. R. Bello, “Design of PV-system with batteries for a grid connected building,” 2017.

[30] M. K. M. L. H. M. Hannu-Pekka Hellman, “Photovoltaic Pover Generation,” in *15th International Scientific Conference of Electric Power Engineering*, Brno, 2014.

[31] “CIBSE Guide A, Environmental design, building services publications, building services knowledge, CIBSE publications,” [Online]. Available: https://www.cibse.org/Knowledge/Guide-A-2015-Supplementary-Files. [Accessed 2018 07 20].

[32] ESRU, “Energy Resources and Policy Handout: Solar power,” 2017. [Online]. Available: http://www.esru.strath.ac.uk/Courseware/Class-ME909-ME922-ME927/Handouts/solar_handout.pdf. [Accessed 20 July 2018].

[33] “Online calculator: Sun position at a given date. Azimuth and elevation table,” [Online]. Available: https://planetcalc.com/4270/. [Accessed 20 July 2018].

[34] “Premium Deep Cycle Batteries | Rolls Battery,” [Online]. Available: http://www.rollsbattery.com/wp-content/uploads/2018/01/Rolls_Battery_Manual.pdf. [Accessed 20 07 2018].

[35] “Parallel Charging Using Multiple Controllers With Separate PV Arrays,” Morningstar, [Online]. Available: https://www.morningstarcorp.com/parallel-charging-using-multiple-controllers-separate-pv-arrays/. [Accessed 1 08 2018].

[36] “Investopedia,” [Online]. Available: https://www.investopedia.com/terms/p/paybackperiod.asp. [Accessed 30 07 2018].

[37] “Corporate Finance Institute,” [Online]. Available: https://corporatefinanceinstitute.com/resources/knowledge/finance/internal-rate-return-irr/. [Accessed 30 07 2018].

[38] “Geothermal Boreholes,” Synergy Boreholes and Systems Ltd, [Online]. Available: http://www.synergyboreholes.co.uk/geothermal_boreholes/index/cost/. [Accessed 29 07 2018].

[39] “Ofgem. Feed-In Tariff (FIT) rates,” [Online]. Available: https://www.ofgem.gov.uk/environmental-programmes/fit/fit-tariff-rates. [Accessed 30 7 2018].

[40] M. Forsen, “Heat Pump- Technology and Environmental Impact,” European Heat Pump Association, 2005.

[41] Department of Energy & Climate Chaange, “Impact of Leakage from Refrigerants in Heat Pumps,” Department of Energy & Climate Change, London, 2014.

[42] Nikolas Hill, Eugenia Bonifazi, Rebekah Bramwell, Eirini Karagianni, Billy Harris, “2018 Government GHG Conversion Factors For Company Reporting,” Department for Business, Energy & Industrial Strategy , London, 2018.

[43] Environment Agency, “Environmental Good Practice Guide for Ground Source Heating and Cooling,” Environment Agency, Bristol.

[44] “Greenhouse Emissions of Solar Panels,” GREENMATCH, [Online]. Available: https://www.greenmatch.co.uk/blog/2015/09/greenhouse-emissions-of-solar-panels. [Accessed 15 08 2018].

[45] G. V. o. B. I. o. P. &. E. A. Occupational Knowledge International, “Health & Environmental Impacts from Lead Battery Manufacturing & Recycling in China,” Occupational Knowledge International, San Francisco, 2011.

[46] L. Concessao, Investigating the Sustainability Performance of Housing Co-operatives using West Whitlawburn Housing Co-operative as a Case Study, Glasgow , 2016.

[47] “www.vent-axia.com,” 2016 September 2016. [Online]. Available: https://www.vent-axia.com/sites/default/files/Ventilation%20Design%20Guidelines%202.pdf. [Accessed 8 July 2018].

[48] CIBSE, “Environmental design. CIBSE Guide A,” The Chartered Institution of Building Services Engineers, London, 2006.

[49] “Hybrid Energy Systems in Future Low Carbon Buildings,” [Online]. Available: http://www.esru.strath.ac.uk/EandE/Web_sites/09-10/Hybrid_systems/esp-r.htm. [Accessed 05 7 2018].

[50] S. J. Rees, Adnvanced in ground-source heat pump systems, Woodhead Publishing, 2016.

[51] M Bernier, M Ahmadfard, “An alternative to ASHRAE's design lenght equation for sizing borehole heat exchangers,” *ASHRAE Transactions,* vol. 120(2).

[52] C. Yavuzturk, “Modeling of Vertical Ground Loop Heat Exchangers for Ground Source Heat Pump Systems,” Berlin, 1988.

[53] KWT Viessman Group, “Heat pumps up to 2000 kW,” 2014. [Online]. Available: https://viessmann.com/com/content/dam/vi-corporate/COM/Download/Heat_pumps_up_to_2000%20kW.pdf/_jcr_content/renditions/original.media_file.download_attachment.file/Heat_pumps_up_to_2000%20kW.pdf. [Accessed 5 July 2018].

[54] British Standards Institution, “Energy performance of buildings- Method for calculation of system energy requirements and system efficiencies,” BSI, London, 2017.

[55] B. S. Institution, “Heating System in Buildings - Method for calculation of system energy requirements and systemn efficiencies Part 4.2: Space heating generation systems, heat pump systems,” BSI, 2008.

[56] T. M. Ahid Irshad, “Report prepared for Solar Scotland, Dumbarton,” Edinburgh Napier University, Edinburgh.

[57] Seung-Hoon Park, Jung-Yeol Kim, Young-Sung Jang, Eui-Jong Kim, “Development of a Multi-Objective Sizing Method for Borehole Heat Exchangers during the Early Design Phase,” *Sustainability ,* vol. 9, 2017.

[58] “Energy Conservation Solution Provider - Renewable Energy and Energy Saving Products and Systems,” Leonics, [Online]. Available: http://www.leonics.com/support/article2_12j/articles2_12j_en.php. [Accessed 2018 06 20].

[59] N. S. &. H. Madani, “Integrating Solar PVT Collectors with GSHP in multi-family houses,” in *12th IEA Heat Pump Conference* , Rotterdam, 2017.

[60] M. B. Massimo Cimmino, “Experimental determination of the g-functions of a small-scale geothermal borehole,” *Geothermics,* p. 61, 2015.

[61] S. Klein, “Calculation of monthly avarage insolation on tiled surfaces,” *Solar Energy,* vol. 19, pp. 325-329, 1976.

[62] Unal Camdali, Murat Bulut, Nedim Sozbir, “Numerical modelling of a ground source heat pump: The Bolu case,” *Renewable Energy,* vol. 83, pp. 252-361, 2015.

[63] “Renergy | 10-35kW | Solar Inverter Datasheet | ENF Inverter Directory,” [Online]. Available: https://www.enfsolar.com/pv/inverter-datasheet/2259. [Accessed 07 2018].

[64] “Annual Fuel Poverty Statistics Report, 2018,” Department for Business,Energy & Industrial Strategy, London, 2018.

[65] Scottish House Condition Survey, “Scottish House Condition Survey: 2016 Key Findings,” The Scottish Goverment, Edinburgh, 2017.

[66] Sustainalble Energy Authority of Irland, “Heat Pump Technologies. Best Practice Guide,” Dublin, 2017.

[67] “nuclear-power,” [Online]. Available: https://www.nuclear-power.net/nuclear-engineering/thermodynamics/thermodynamic-cycles/heating-and-air-conditioning/coefficient-of-performance-cop-refrigerator-air-conditioner/. [Accessed 20 06 2018].

[69] K. R. Steve Kavanaugh, Gheothermal Heating and Cooling, Atlanta: ASHRAE, 2014.

[70] “Kynix Semicinductor Electronic Blog,” [Online]. Available: http://www.apogeeweb.net/article/27.html. [Accessed 15 07 2018].

[71] [Online]. Available: https://www.vecteezy.com/vector-art/99723-heat-pump-system.

[73] N. Sommerfiel.

[74] ESRU, “Energy Resources and Policy Lecture: Solar Power,” [Online]. Available: http://www.esru.strath.ac.uk/Courseware/Class-ME909-ME922-ME927/Presentations/solar.pdf. [Accessed 10 07 2018].

[75] M. Bernier, “Bore Field sizing: Theory and applications,” Politechnique Montreal, Montreal , 2015.

[76] Nelson Sommerfield, Hatef Madani, “Integrating Solar PVT Collectors With GSHP In Multi-Family Houses,” Rotterdam, 2017.